

---

# INTRODUCTION TO QUANTUM MECHANICS

A Time-Dependent Perspective

David J. Tannor  
Weizmann Institute of Science



UNIVERSITY SCIENCE BOOKS  
Sausalito, California

# Chapter 11

---

## Numerical Methods for Solving the Time-Dependent Schrödinger Equation

The formal framework for quantum mechanics is an infinite dimensional Hilbert space. In any numerical calculation, however, it is necessary to truncate the basis at some finite dimension,  $N$ . An elegant way of thinking about the dynamics on this reduced Hilbert space is that the reduced space *could*, in principle, be the complete space for a different quantum mechanical problem. Therefore, why not demand that all the usual formalism of quantum mechanics apply on this reduced Hilbert space, for example, orthogonality relations, completeness relations, unitary transformations and so forth. In favorable cases we may even expect that commutator relations and the uncertainty principle may take the same form as on the full Hilbert space. The key to providing a rigorous formulation of the quantum dynamics on the reduced Hilbert space is to realize that the truncation to  $N$  basis functions can be described by a projection operator,  $P_N$ , projecting onto the space spanned by the basis. The Hamiltonian viewed as a mapping on this subspace (see Section 11.1) becomes

$$H_N = P_N H P_N = P_N T P_N + P_N V P_N \quad (11.1)$$

and the Time-Dependent Schrödinger Equation becomes

$$i\hbar \frac{\partial \Psi_N}{\partial t} = H_N \Psi_N, \quad (11.2)$$

where  $\Psi_N(t=0) = P_N \Psi(t=0)$ .

However, the most prevalent methods for solving the TDSE today do not use conventional orthogonal bases, but rather grid representations: a continuous wavefunction is represented in terms of a discrete set of time-evolving complex amplitudes at a set of grid points. What relationship, if any, is there between the representation in terms of complex amplitudes at grid points and a representation in terms of a conventional basis of orthogonal functions? As will be shown in this chapter, the amplitudes at the grid points can be interpreted as the coefficients of localized basis functions. The conventional basis of orthogonal functions is referred to as a “spectral” basis, while the basis of localized functions is called a “pseudospectral” basis. If these two bases are related by a unitary transformation, the projection operators associated with the two bases are identical. As a result, completeness relations on the subspace that can be expressed in terms of the spectral basis can be expressed in terms of the pseudospectral basis as well. It is usually convenient to evaluate the kinetic energy,  $T_N$ , in a spectral basis, and the potential energy,  $V_N$ , in a pseudospectral

basis. Ultimately, a single representation has to be chosen for  $H_N = T_N + V_N$ , but this is easily accomplished provided the unitary transformation between the two representations is known. The equivalence of the projection operators in the two representations guarantees that the reduced Hilbert space on which  $H$  is represented is defined consistently. Two important examples of this combination of spectral and pseudospectral representation are the Fourier method and the DVR (discrete variable representation) method, both of which will be described in detail in this chapter.

In addition to the projection onto a subspace of the Hilbert space associated with  $P_N$ , there is a second source of numerical error, coming from the approximate evaluation of the operators within this reduced Hilbert space. For the systems of interest in this chapter,  $T_N$  can be calculated *exactly* in the spectral basis, using derivative relations for the orthogonal functions; however, the calculation of  $V_N$  is generally approximate. Consider the evaluation of  $V_N$  in the spectral representation. Each element involves integrals of the form  $\int \phi_m^*(x) V(x) \phi_n(x) dx$ , with  $V(x)$ ,  $\phi_m$  and  $\phi_n$  normally quite complicated, and hence in general the integral cannot be evaluated analytically. However, if  $V_N$  is represented in a pseudospectral basis, the matrix elements now involve integrals of products of the complicated  $V(x)$  with *localized* basis functions. The simple procedure of essentially treating the pseudospectral basis functions as if they were  $\delta$ -functions turns out to be remarkably accurate, leading to a diagonal representation of  $V_N$  whose elements are simply the value of  $V(x)$  at the position of the associated  $\delta$ -function. As we shall show in this chapter, this approximation can be described formally by the replacement

$$P_N V(\hat{x}) P_N = V_N(\hat{x}) \rightarrow V(\hat{x}_N) = V(P_N \hat{x} P_N). \quad (11.3)$$

The representation of  $T_N$ , while not diagonal or banded in the pseudospectral basis, is still straightforward to calculate by applying an appropriate unitary transformation to the  $T_N$  in the spectral representation. Combining the two approximations to the Hamiltonian—the projection onto a subspace and the evaluation of the matrix elements—we have

$$H_N \approx T_N(\hat{p}) + V_N(\hat{x}_N). \quad (11.4)$$

Finally, there is a third source of numerical error. This arises because the evaluation of the evolution operator,  $U(t)\psi = e^{-iHt/\hbar}\psi = e^{-i(\hat{p}^2/2m+V(\hat{x}))t/\hbar}\psi$ , is more complicated than evaluation of  $H\psi$ , since in the former the  $x$  and  $p$  operators are entangled through the exponentiation. There are several major approaches to evaluating the evolution operator. One approach is to construct the  $H$  matrix and diagonalize it, that is,  $e^{-iHt/\hbar}\psi = Ue^{-i\lambda t/\hbar}U^{-1}\psi$ . Then propagation is simple, but the price is that diagonalization is expensive. Alternatively, the  $H$  matrix can be used to integrate the Time-Dependent Schrödinger Equation via repeated evaluation of  $H\psi$  to find  $\dot{\psi}$ . This can be accomplished via several methods, for example, by rewriting the Time-Dependent Schrödinger Equation in a form that displays the symplectic (i.e., canonical) structure of classical mechanics and employing well-developed integrators for the classical problem. A second approach, called the Split Operator method, approximates  $e^{-i(\hat{p}^2/2m+V(\hat{x}))t/\hbar}\psi \approx e^{-i(\hat{p}^2 t/2m\hbar)}e^{-iV(\hat{x})t/\hbar}\psi$ . A third class of approaches evaluates  $H\psi$ , and then represents  $e^{-iHt/\hbar}\psi = \sum_n a_n P_n(H)\psi$ , avoiding diagonalization;  $P_n(H)$  is some polynomial of the Hamiltonian operator, whose operation on  $\psi$  can be evaluated by iterative operations of  $H$  on  $\psi$ . Many choices of  $P_n(H)$

are possible; the different possibilities can be divided into two types, those that specify the polynomials in advance (uniform methods) and those that do not (nonuniform methods).

In addition to the formal treatment of numerical methods, and the error incurred, one of the goals of this chapter is to provide a practical guide to the most commonly used algorithms. The reader will find the central equations, for example, for the DVR method, the Fourier Grid Hamiltonian method, the FFT method, the Split Operator method, and the Chebyshev method in Sections 11.5–11.7.

## 11.1 Spectral Projection and Collocation

### 11.1.1 Spectral Projection

#### Preliminaries

A spectral representation refers to the representation of a wavefunction and the operators that act on it in terms of a basis set of orthogonal functions. Because any numerical representation is inherently finite, the infinite set of orthogonal functions must necessarily be truncated at a finite value,  $N$ . This truncation can be expressed in terms of a projection operator,

$$P_N = \sum_{n=1}^N |\phi_n\rangle\langle\phi_n|, \quad (11.5)$$

which projects the dynamics onto an  $N$ -dimensional subspace of the infinite Hilbert space.

Consider, for example, constructing a matrix representation of the Hamiltonian,

$$H = \hat{p}^2/2m + V(\hat{x}), \quad (11.6)$$

using a set of  $N$  orthogonal basis functions. Assume also that the matrix elements  $\langle\phi_m|H|\phi_n\rangle$  are known exactly. Truncation of the matrix  $H$  at  $N \times N$  can be expressed in terms of the projection operator  $P_N$  as

$$H_N = P_N H P_N = T_N + V_N. \quad (11.7)$$

Defining  $Q_N = \mathbf{1} - P_N$ , the TDSE may be written as a set of two coupled differential equations:

$$i\hbar \frac{\partial \Psi_N}{\partial t} = P_N H P_N \Psi_N + P_N H Q_N \Psi_\perp \quad (11.8)$$

$$i\hbar \frac{\partial \Psi_\perp}{\partial t} = Q_N H P_N \Psi_N + Q_N H Q_N \Psi_\perp, \quad (11.9)$$

where  $\Psi_N = P_N \Psi$  and  $\Psi_\perp = Q_N \Psi = \Psi - \Psi_N$ . We will consider in this chapter only numerical methods that neglect the contribution from  $\Psi_\perp$ . In the numerical analysis literature this is known as the Galerkin approximation (see, e.g., Gottlieb, 1977) and corresponds to the solution of the time-dependent variational formulation of the Schrödinger equation in a finite basis described in Section 9.6. If the contribution of  $\Psi_\perp$  is neglected, the TDSE takes the form

$$i\hbar \frac{\partial \Psi_N}{\partial t} = P_N H P_N \Psi_N, \quad (11.10)$$

and in integral form becomes

$$\Psi_N(t) = e^{-iH_N t/\hbar} \Psi_N(0) = e^{-iP_N H P_N t/\hbar} \Psi_N(0) \approx P_N e^{-iH t/\hbar} P_N \Psi(0). \quad (11.11)$$

The approximation in Eq. 11.11 is exact if  $[P_N, H] = 0$ . If the basis functions  $\phi_n$  were the exact eigenfunctions of  $H$ , the commutator  $[P_N, H]$  would indeed be 0; to the extent that the basis functions are close to the exact eigenfunctions the approximation is a reasonable one. Diagonalizing  $H_N$  gives energies  $E_n^N$  and eigenstates  $\psi_n^N$ , which approximate the true energies  $E_n$  and eigenstates  $\psi_n$ . Propagation of the wavepacket using these approximate energies gives

$$\Psi_N(t) = \sum_{n=1}^N a_n^N \psi_n^N e^{-iE_n^N t/\hbar}. \quad (11.12)$$

Equation 11.12 is an example of a “spectral” propagation method, “spectral” referring to a basis of orthogonal eigenstates.

► **Exercise 11.1** Derive Eq. 11.12.

### Phase Space Interpretation of the Reduced Hilbert Space Projection Operator

Every spectral method, and hence every pseudospectral method (Section 11.2 and Eq. 11.49), can be given a phase space interpretation. Once a choice of basis functions is made this defines a projection operator for a subspace of the Hilbert space,

$$P_N = \sum_{n=1}^N |\phi_n\rangle\langle\phi_n|. \quad (11.13)$$

The Wigner transform of the projection operator gives a representation of the region of phase space spanned by the basis

$$P_N^W(p, q) = \sum_{n=1}^N \frac{1}{2\pi\hbar} \int_{-\infty}^{\infty} \phi_n^* \left( q - \frac{s}{2} \right) \phi_n \left( q + \frac{s}{2} \right) e^{ips/\hbar} ds. \quad (11.14)$$

If the basis spans the lowest  $N$  eigenstates of a Hamiltonian, one expects intuitively that the Wigner function of the projection operator will be a function of uniform density 1 in regions below  $H(p, q) \approx E_n$  and of uniform density 0 in regions above  $H(p, q) \approx E_n$ , with a smooth transition region in between, where  $H(p, q)$  is the *classical* Hamiltonian function. Numerical tests show that this is approximately true, although oscillations persist in the interior region of phase space as may be seen in Figure 11.1 (Poirier, 2000).

### The Spectral Projector Acting on a Wavefunction

We now consider the action of a spectral projection operator on a wavefunction. Although these results are simple and straightforward we present them here in order to contrast them with the action of the collocation projection operator in Section 11.1.2, which is most easily understood in terms of its action on a wavefunction.

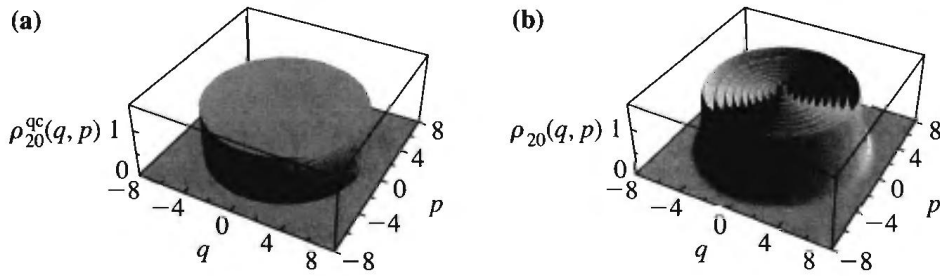


**Figure 11.1** Phase space distributions  $\rho(p, q)$  corresponding to the projection operator  $P_N = \sum_{n=1}^N |\phi_n\rangle\langle\phi_n|$  for the one-dimensional harmonic oscillator  $H(p, q) = (q^2 + p^2)/2$  with  $N = 20$ . (a) quasiclassical distribution; (b) exact quantum distribution based on the Wigner representation of the projection operator, Eq. 11.14. Adapted from Poirier (2000).

Consider an arbitrary wavefunction  $\psi(x)$ . We may decompose  $\psi(x)$  in terms of an infinite, orthonormal basis  $\{\phi_n\}$  as follows:

$$\psi(x) = \sum_{n=1}^{\infty} a_n \phi_n(x), \quad (11.15)$$

where

$$\int \phi_m^*(x) \phi_n(x) dx = \delta_{mn}, \quad a_n = \int \phi_n^*(x) \psi(x) dx, \quad m, n = 1, \dots, \infty. \quad (11.16)$$

We define the spectral projection operator  $P_N$  such that

$$\tilde{\psi}(x) = P_N \psi(x) = \sum_{n=1}^N a_n \phi_n(x), \quad (11.17)$$

with  $a_n$  given by Eq. 11.16 for  $n = 1, \dots, N$ . It is easy to show that

$$P_N \phi_n(x) = \begin{cases} \phi_n(x) & n = 1, \dots, N \\ 0 & n = N+1, \dots \end{cases} \quad (11.18)$$

It follows that  $P_N^2 = P_N$ :

$$P_N^2 \psi(x) = P_N \sum_{n=1}^N a_n \phi_n(x) = \sum_{n=1}^N a_n P_N \phi_n(x) = \sum_{n=1}^N a_n \phi_n(x) = P_N \psi(x). \quad (11.19)$$

► **Exercise 11.2** Show that  $P_N = \sum_{n=1}^N |\phi_n\rangle\langle\phi_n|$  satisfies Eq. 11.17 with  $a_n$  given by Eq. 11.16. We have used a more cumbersome notation in Eqs. 11.16 and 11.17 in anticipation of our discussion of the collocation projector.

### 11.1.2 Collocation

#### Definition of the Collocation Projector

Collocation refers to the numerical solution of a set of equations such that the result is exact at a discrete set of points. One can associate with collocation a projection operator defined as follows:

$$\tilde{\psi}(x) = P_N \psi(x) = \sum_{n=1}^N b_n \phi_n(x), \quad (11.20)$$

where the  $b_n$  are determined by the condition that  $\tilde{\psi}(x) = \psi(x)$  at the  $N$  collocation points  $\{x_i\}$ ,  $i = 1, \dots, N$ , that is,

$$\tilde{\psi}(x_i) = P_N \psi(x_i) = \sum_{n=1}^N b_n \phi_n(x_i) = \psi(x_i) \quad i = 1, \dots, N. \quad (11.21)$$

Equation 11.21 defines an interpolation scheme at points other than the collocation points via the relation

$$\tilde{\psi}(x) = \sum_{n=1}^N b_n \phi_n(x) \approx \psi(x). \quad (11.22)$$

Consider now the action of  $P_N^2$ :

$$P_N^2 \psi(x_i) = P_N \tilde{\psi}(x_i) = \sum_{m=1}^N c_m \phi_m(x_i), \quad (11.23)$$

where Eq. 11.23 defines the  $\{c_n\}$ . But from Eq. 11.21  $P_N \tilde{\psi}(x_i) = \tilde{\psi}(x_i)$  and hence

$$P_N^2 \psi(x_i) = P_N \tilde{\psi}(x_i) = \tilde{\psi}(x_i) = \sum_{n=1}^N b_n \phi_n(x_i). \quad (11.24)$$

For Eqs. 11.23 and 11.24 to be consistent we must have  $c_n = b_n$ ,  $n = 1, \dots, N$  and hence  $P_N^2 = P_N$ .

Equation 11.21 can be written in matrix form as

$$\bar{\Psi} = \Phi \mathbf{b} \quad (11.25)$$

where  $\bar{\Psi}_j = \psi(x_j)$  and the matrix elements are  $\Phi_{jn} = \phi_n(x_j)$ . Provided that the  $\phi_n(x_j)$  are linearly independent, the solution is

$$\mathbf{b} = \Phi^{-1} \bar{\Psi}. \quad (11.26)$$

One of the principal properties of the collocation projection is that it obeys a composition property

$$\tilde{\psi}_1(x) \tilde{\psi}_2(x) = \widetilde{\psi_1 \psi_2}(x). \quad (11.27)$$

► **Exercise 11.3** Verify Eq. 11.27.

### Contrasting the Spectral and Collocation Projectors: Orthogonal versus Nonorthogonal Projection

We now observe that  $P_N$  for both spectral projection and collocation project onto the same subspace of the Hilbert space, which we may call  $\mathcal{H}_N \equiv \text{span}\{\phi_1, \dots, \phi_N\}$ . The two projectors differ not in the space onto which they project but in the state that they produce in the reduced subspace, which manifests itself in terms of the difference in the coefficients  $\{a_n\}$

versus  $\{b_n\}$ . The difference in the state produced can be given a geometrical interpretation as follows. Define the quantity

$$\chi = \psi - \tilde{\psi}. \quad (11.28)$$

For spectral projection we have

$$\chi(x) = \sum_{n=1}^{\infty} a_n \phi_n(x) - \sum_{n=1}^N a_n \phi_n(x) = \sum_{n=N+1}^{\infty} a_n \phi_n(x). \quad (11.29)$$

It is easily seen that  $\langle \chi | \tilde{\psi} \rangle = 0$ :

$$\langle \chi | \tilde{\psi} \rangle = \int \left( \sum_{n=N+1}^{\infty} a_n^* \phi_n^*(x) \right) \left( \sum_{m=1}^N a_m \phi_m(x) \right) dx = 0. \quad (11.30)$$

The orthogonality of the residue  $\chi$  to the projected part of the state,  $\tilde{\psi}$ , shows that the spectral projector is an *orthogonal projector*. Now consider the collocation projector. In this case the residue becomes

$$\chi(x) = \sum_{n=1}^{\infty} a_n \phi_n(x) - \sum_{n=1}^N b_n \phi_n(x). \quad (11.31)$$

Now  $\langle \chi | \tilde{\psi} \rangle \neq 0$ :

$$\langle \chi | \tilde{\psi} \rangle = \int \left( \sum_{n=1}^N (a_n - b_n)^* \phi_n^*(x) \right) \left( \sum_{m=1}^N b_m \phi_m(x) \right) dx \neq 0. \quad (11.32)$$

The collocation projector is a *nonorthogonal projector*. The fact that two projectors can project a vector onto the same subspace but produce two different vectors is shown geometrically in Figure 11.2.

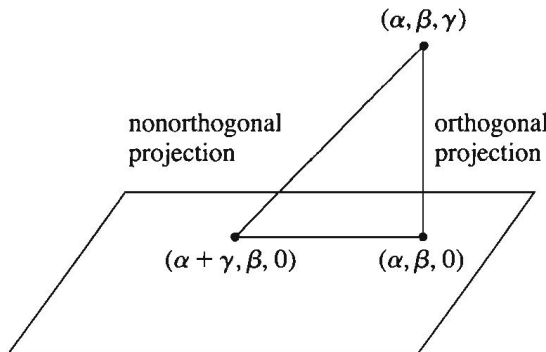


**Figure 11.2** Geometrical interpretation of orthogonal and nonorthogonal projection from a three-dimensional to a two-dimensional Euclidean space. Note that both the orthogonal and nonorthogonal projectors have no  $z$ -component in the final vector. In the orthogonal projection, the  $z$ -component in no way influences the value of  $x$  or  $y$  in the final vector, while in the nonorthogonal projection it does.

---

► Exercise 11.4

- a. Show that both

$$\mathbf{P}_1 = \begin{pmatrix} 1 & 0 & 0 \\ 0 & 1 & 0 \\ 0 & 0 & 0 \end{pmatrix} \quad \text{and} \quad \mathbf{P}_2 = \begin{pmatrix} 1 & 0 & 1 \\ 0 & 1 & 0 \\ 0 & 0 & 0 \end{pmatrix} \quad (11.33)$$

satisfy the relationship  $\mathbf{P}^2 = \mathbf{P}$ , but only the first is Hermitian. The Hermitian character of the matrix is the signature of an orthogonal projection.

- b. Calculate the action of  $\mathbf{P}_1$  and  $\mathbf{P}_2$  on the column vector  $(\alpha, \beta, \gamma)^T$ . What happens to the third component of the *final* vector under orthogonal projection? Under nonorthogonal projection? What happens to the third component of the *initial* vector under orthogonal projection? Under nonorthogonal projection? Interpret your result geometrically using Figure 11.2.

► Exercise 11.5

- a. Show that if  $\psi(x)$  lies within the projected Hilbert space, that is,  $\psi(x) = \sum_{n=1}^N a_n \phi_n(x)$ , then  $\tilde{\psi}(x)$  for spectral projection and for collocation give the same result.
- b. Show that the  $\{a_n\}$  in both spectral projection and collocation satisfy the relationship

$$a_n = \int \phi_n^*(x) \tilde{\psi}(x) dx \quad (11.34)$$

(note that  $\tilde{\psi}(x)$  and not  $\psi(x)$  appears on the RHS).

---

### Orthogonal Collocation

Is it possible for a projector that satisfies the collocation conditions exactly to also be an orthogonal projector? Consider the case that the expansion functions  $\phi_n(x)$  obey a set of discrete orthogonality relations at the collocation points:

$$\sum_{j=1}^N \phi_m^*(x_j) \phi_n(x_j) \Delta_j = \delta_{mn}, \quad m, n = 1, \dots, N. \quad (11.35)$$

Equation 11.35 represents a set of orthogonality relations that are analogous to those of Eq. 11.16, with the integral replaced by a sum over values at the collocation points,  $x_j$ , and  $dx$  replaced by a generally  $j$ -dependent weight factor  $\Delta_j$ . Despite the flexibility in choosing the points  $\{x_j\}$  and the weights  $\{\Delta_j\}$ , Eq. 11.35 is nontrivial to satisfy: the same points and weights must simultaneously satisfy all the orthogonality relations for  $1 \leq m, n \leq N$ .

Equation 11.35 allows for direct inversion of the coefficients  $b_n$  in Eq. 11.21 by left multiplying by  $\phi_m^*(x_j) \Delta_j$  and summing over  $j$ :

$$b_n = \sum_{j=1}^N \psi(x_j) \phi_n^*(x_j) \Delta_j. \quad (11.36)$$

With the  $\{b_n\}$  chosen according to Eq. 11.36 the conditions for collocation are satisfied precisely. Yet clearly Eq. 11.36 is also a discrete approximation to the relation  $a_n = \int \phi_n^*(x) \psi(x) dx$ , which according to Eq. 11.16 is the condition for an orthogonal

projection! Because Eq. 11.36 is only an approximation to the integral Eq. 11.16, it does not exactly define an orthogonal projection; nevertheless, because it provides a close approximation we will refer to schemes satisfying the property 11.35 (and hence 11.36) as orthogonal collocation schemes.

Orthogonal collocation schemes can be recast in a simple and powerful way. We begin by defining

$$\Phi_n(x_j) \equiv \sqrt{\Delta_j} \phi_n(x_j). \quad (11.37)$$

With this definition Eq. 11.35 can be written as

$$\sum_{j=1}^N \Phi_m^*(x_j) \Phi_n(x_j) = \delta_{mn} \quad 1 \leq m, n \leq N. \quad (11.38)$$

Defining  $\Phi_n(x_j) \equiv \Phi_{jn}$  we may rewrite Eq. 11.38 in matrix notation as

$$\Phi^\dagger \Phi = \mathbf{1}. \quad (11.39)$$

Equation 11.39 indicates that the transformation matrix  $\Phi$  is unitary. The unitarity of the transformation implies a second relation:

$$\Phi \Phi^\dagger = \mathbf{1}, \quad (11.40)$$

or in component form

$$\sum_{n=1}^N \Phi_n(x_i) \Phi_n^*(x_j) = \delta_{ij} \quad 1 \leq i, j \leq N. \quad (11.41)$$

Despite the apparent similarity between Eq. 11.41 and Eq. 11.38, the physical significance is completely different. Equation 11.41 is effectively an orthogonality relation for the different grid points, the analog of the relation

$$\langle x' | x \rangle = \sum_{n=1}^{\infty} \langle x' | n \rangle \langle n | x \rangle = \delta(x - x') \quad (11.42)$$

on the infinite Hilbert space. Below, we will refer to  $\Phi$  as the orthogonal collocation matrix. Relations of the type in Eq. 11.39 will be referred to as basis orthogonality relations and relations of the type in Eq. 11.40 as grid orthogonality relations. The grid orthogonality relation, Eq. 11.41, is the starting point for our discussion of the pseudospectral basis in the next section.

## 11.2 The Pseudospectral Basis

### 11.2.1 Definition of the Pseudospectral Basis

Although we have defined the projection operator  $P_N$  in Eq. 11.5 in terms of the basis  $\{\phi_n\}$ ,  $P_N$  is an operator and therefore formally basis independent. This hints that  $P_N$  may be represented in a basis other than the spectral basis without any loss of accuracy, provided that the new basis is related to the spectral basis by a unitary transformation on the reduced Hilbert space.

An important special case is the representation of  $P_N$  in a pseudospectral basis—a basis of spatially *localized* functions, each one concentrated around a different spatial center. Collectively, the  $N$  pseudospectral basis functions  $\{\theta_j\}$  span *exactly* the same Hilbert space as the  $N$  spectral basis functions from which they derive via a unitary (or orthogonal) transformation. Hence the projector in the pseudospectral basis is fundamentally identical to the projector in the spectral basis,

$$P_N = \sum_{n=1}^N |\phi_n\rangle\langle\phi_n| = \sum_{j=1}^N |\theta_j\rangle\langle\theta_j|.$$

The major properties of the pseudospectral representation will be derived in this section.

It is interesting to see the pseudospectral basis emerge from the theory of orthogonal collocation. If we replace  $\Phi_n(x_i) \rightarrow \phi_n(x)$  in only the first factor in Eq. 11.41 we obtain

$$\sum_{n=1}^N \phi_n(x) \Phi_n^*(x_j) \equiv \theta_j(x), \quad (11.43)$$

where we have defined the pseudospectral basis functions,  $\{\theta_j(x)\}$ . Because the LHS of Eq. 11.43 is in some sense close to the LHS of Eq. 11.41, we expect the functions  $\{\theta_j(x)\}$  to be close to  $\delta$ -functions. In fact, the functions  $\{\theta_j\}$  are localized, each one around a different value of  $x_j$ . Moreover, they satisfy the modified Kronecker  $\delta$ -function property

$$\theta_j(x_i) = \Delta_j^{-1/2} \delta_{ij}, \quad (11.44)$$

as follows immediately from Eq. 11.43 together with Eqs. 11.37 and 11.41. Illustrations of the functions  $\theta_j(x)$  may be seen later in the chapter in Figures 11.4 and 11.6.

Equation 11.43 can be written in matrix–vector notation as

$$\Phi^\dagger \phi(x) = \theta(x), \quad (11.45)$$

showing that the functions  $\{\theta_j(x)\}$  can be viewed as an alternative basis to the original basis  $\{\phi_n\}$ . Because the basis  $\{\theta_j\}$  and the original basis  $\{\phi_n\}$  are related by a unitary transformation  $\Phi^\dagger$ , they project onto the same subspace of the Hilbert space. Thus, every unitary (or in the case of real basis functions, orthogonal) collocation relation of the form in Eq. 11.38 implies the existence of a set of localized basis functions that span the same space as the original orthogonal functions; the form of the localized basis is determined completely by the points and weights that enter into Eq. 11.38, and the primary basis of orthogonal functions  $\{\phi_n\}$ .

### 11.2.2 Completeness and Orthogonality of Pseudospectral Basis Functions

The localized basis functions  $\theta_n$  have properties of completeness and orthogonality entirely analogous to those of the original basis,  $\phi$ . To show this, we first invert Eq. 11.43 by multiplying by  $\phi_m^*(x)$  and integrating over the domain. This gives

$$\Phi_n^*(x_j) = \langle \phi_n | \theta_j \rangle. \quad (11.46)$$

The grid orthogonality relation, Eq. 11.41, then becomes

$$\sum_{n=1}^N \Phi_n(x_i) \Phi_n^*(x_j) = \delta_{ij} = \sum_{n=1}^N \langle \theta_i | \phi_n \rangle \langle \phi_n | \theta_j \rangle = \langle \theta_i | \theta_j \rangle. \quad (11.47)$$

Similarly, the basis orthogonality relation, Eq. 11.38, becomes

$$\sum_{j=1}^N \Phi_m^*(x_j) \Phi_n(x_j) = \delta_{mn} = \sum_{j=1}^N \langle \phi_m | \theta_j \rangle \langle \theta_j | \phi_n \rangle. \quad (11.48)$$

Equation 11.47 is a statement of the orthonormality of the different  $\theta$  basis functions. This orthogonality may be understood qualitatively, given that each  $\theta$  function is peaked around a different value of  $x_i$  and vanishes at all other values  $x_j$ , but the precise orthogonality includes the cancellation of the oscillatory portions of the  $\theta$  functions away from the peak as well. Equation 11.48 is a completeness (or closure) relationship with respect to summation over all the grid points  $j$ . The property of completeness says in essence that representation onto the localized  $\theta$  functions represents projection onto the exact same subspace of Hilbert space as the projection defined by the original basis of orthogonal functions. Both the completeness and orthogonality of the  $\theta$  functions follow immediately from the fact that the transformation matrix with elements  $\Phi_n(x_i)$  is unitary. Thus, the formal statement of the closure relation is

$$P_N = \sum_{n=1}^N |\phi_n\rangle\langle\phi_n| = \sum_{j=1}^N |\theta_j\rangle\langle\theta_j|. \quad (11.49)$$

Consider applying the projection operator  $P_N$  to a Dirac delta function:

$$P_N \delta(x - x_i) = \sum_{j=1}^N \langle x | \theta_j \rangle \langle \theta_j | x_i \rangle = \Delta_i^{-1/2} \theta_i(x), \quad (11.50)$$

where we have used Eq. 11.44. Equation 11.50 indicates that the functions  $\{\theta_i\}$  can be viewed as “smeared” delta functions that approach actual delta functions in the limit that the size of the basis goes to infinity.

### 11.2.3 The Collocation Projector in the Pseudospectral Basis

We now return to the collocation relation, Eq. 11.20. Note that Eq. 11.43 can be inverted to give

$$\phi_n(x) = \sum_{i=1}^N \Phi_n(x_i) \theta_i(x), \quad (11.51)$$

or in matrix–vector notation

$$\Phi \theta(x) = \phi(x). \quad (11.52)$$

Using this relation we can rewrite the collocation relation as

$$\tilde{\psi}(x) = \sum_{n=1}^N b_n \phi_n(x) = \sum_{i=1}^N \left\{ \sum_{n=1}^N b_n \Phi_n(x_i) \right\} \theta_i(x) \quad (11.53)$$

$$= \sum_{i=1}^N \psi(x_i) \theta_i(x) \Delta_i^{1/2} \approx \psi(x), \quad (11.54)$$

where we have used Eqs. 11.21 and 11.37. At the collocation points  $\{x_i\}$  we have

$$\tilde{\psi}(x_i) = \sum_{i=1}^N \psi(x_i) \theta_i(x_i) \Delta_i^{1/2} = \psi(x_i). \quad (11.55)$$

Comparing Eq. 11.55 with Eq. 11.21 we see that it is a collocation formula with the basis functions  $\{\theta_i\}$  replacing  $\{\phi_n\}$ . The coefficients of the basis functions are the values of the exact function  $\psi(x)$  at the collocation points  $\{x_i\}$ —the same points as in the collocation expression using  $\{\phi_n\}$ —with a weight factor of  $\Delta_i^{1/2}$ .

Multiplying both sides of Eq. 11.54 by  $\theta_j(x)$  and integrating we obtain

$$\langle \theta_j | \tilde{\psi} \rangle = \sum_{i=1}^N \psi(x_i) \langle \theta_j | \theta_i \rangle \Delta_i^{1/2} = \psi(x_j) \Delta_j^{1/2}. \quad (11.56)$$

The significance of Eq. 11.56 is that for any state  $\tilde{\psi}$  that is in the space  $\mathcal{H}_N$ , its inner product with the  $\theta$  function centered at point  $x_i$  is just given by the value of  $\tilde{\psi}$  at the point  $x_i$  multiplied by a number that depends on the point but not on the function  $\tilde{\psi}$ .

With the aid of Eq. 11.54 we can derive a simple formula for the collocation projector in Dirac notation. We have

$$\langle x | \tilde{\psi} \rangle = \sum_{i=1}^N \psi(x_i) \theta_i(x) \Delta_i^{1/2} \quad (11.57)$$

$$= \sum_{i=1}^N \langle x | \theta_i \rangle \langle x_i | \psi \rangle \Delta_i^{1/2}. \quad (11.58)$$

But  $\langle x | \tilde{\psi} \rangle = \langle x | P_N | \psi \rangle$  so we see from Eq. 11.58 that the collocation projector may be written formally as

$$P_N = \sum_{i=1}^N |\theta_i\rangle \langle x_i| \Delta_i^{1/2}. \quad (11.59)$$

#### ► Exercise 11.6

- a. Show that  $P_N$  given by Eq. 11.59 satisfies the properties  $P_N^2 = P_N$  but  $P_N^\dagger \neq P_N$ , consistent with  $P_N$  for collocation being a nonorthogonal projector.
- b. Use Eq. 11.59 to show the composition property of collocation projection  $\tilde{\psi}_1 \tilde{\psi}_2 = \widetilde{\psi_1 \psi_2}$  (cf. Exercise 11.3).

#### 11.2.4 Evaluation of Integrals by Sampling at Collocation Points

Now consider the inner product  $\langle \tilde{\psi}_1 | \tilde{\psi}_2 \rangle$ . Using the form for the collocation projector, Eq. 11.59, we may obtain a simple result about the exactness of evaluating this integral by evaluating the integrand at the collocation points. In particular,

$$\langle \tilde{\psi}_1 | \tilde{\psi}_2 \rangle = \langle \tilde{\psi}_1 | P_N^\dagger P_N | \tilde{\psi}_2 \rangle = \sum_{i,j=1}^N \langle \tilde{\psi}_1 | x_j \rangle \langle \theta_j | \theta_i \rangle \langle x_i | \tilde{\psi}_2 \rangle \Delta_i^{1/2} \Delta_j^{1/2} \quad (11.60)$$

$$= \sum_i^N \langle \tilde{\psi}_1 | x_i \rangle \langle x_i | \tilde{\psi}_2 \rangle \Delta_i = \sum_{i=1}^N \tilde{\psi}_1^*(x_i) \tilde{\psi}_2(x_i) \Delta_i, \quad (11.61)$$

where we have used Eqs. 11.59 and 11.47. Equation 11.61 says that the evaluation of the inner product of two functions that lie within the Hilbert space  $\mathcal{H}_N$  is exact if the integrand is evaluated at the collocation points and summed with the weighting factor  $\Delta_i$ . The key step in the derivation is inserting  $P_N^\dagger$  and  $P_N$  in the first step; this is permissible since both  $\tilde{\psi}_1$  and  $\tilde{\psi}_2$  lie within the space  $\mathcal{H}_N$  and for functions within this space the collocation projector is transparent. One may show that Eq. 11.61 implies that

$$\int f(x) dx = \sum_{i=1}^N f(x_i) \Delta_i \quad (11.62)$$

for  $f(x)$  in  $\mathcal{H}_{2N-1}$ . Equation 11.62 is a remarkable result. It indicates that with just  $N$  quadrature points and weights we can evaluate exactly the integral of any function that exists within the associated  $2N - 1$  dimensional Hilbert space.

### 11.3 Gaussian Quadrature

A major component of our exposition of pseudospectral methods and their accuracy was the assumption of an orthogonal collocation relation of the form of Eq. 11.35. But we have not discussed how one might go about finding the points  $\{x_i\}$  and weights  $\{\Delta_i\}$  that will simultaneously make the set of  $N^2$  orthonormality relations hold. For a Fourier basis the points and weights can be guessed intuitively: the points are evenly spaced and the weights at every point are equal. However, for a general basis of orthogonal functions it is not obvious how to find the points and weights. We will present here a method to find the points and weights for a basis of orthogonal functions based on the classical polynomials. It turns out that, in addition to allowing the points and weights for orthogonal collocation to be found in a fully automatic way, there is an additional bonus: the evaluation of inner products using the collocation points and weights is exact provided that the integrand lies within  $\mathcal{H}_{2N}$ , rather than just  $\mathcal{H}_{2N-1}$ .

The property that an integral can be evaluated exactly for an integrand lying within a  $2N$ -dimensional Hilbert space using only  $N$  points and weights is the characteristic feature of integration by Gaussian quadrature integration. In what follows, we will show explicitly the connection between the method presented for finding orthogonal collocation points and weights and the theory of Gaussian quadrature. In Section 11.3.1 we will begin by assuming

the existence of Gaussian quadrature points and weights. In Section 11.3.3 we will show that the theory of Gaussian quadrature can actually be derived from first principles from the properties of the pseudospectral functions.

### 11.3.1 Quadrature Points and Weights by Matrix Diagonalization

We begin with a brief statement of the main results of the theory of Gaussian quadrature. Consider approximating the integral of a function  $f(x)$  by a finite sum:

$$\int_a^b w(x) f(x) dx \approx \sum_{i=1}^N W_i f(x_i), \quad (11.63)$$

where  $w(x)$  is a positive weight function and the  $N$  values  $\{W_i\}$  are the weights to be given to the  $N$  function values  $f(x_i)$ . If the points are not fixed there are  $2N$  undetermined parameters (the  $\{W_i\}$  and the  $\{x_i\}$ ), precisely the number of parameters needed to determine a polynomial of degree  $2N - 1$  (the extra parameter is needed to determine the constant term in the polynomial). In Gaussian quadrature, the  $\{x_i\}$  and the  $\{W_i\}$  are chosen such that the sum in Eq. 11.63 yields the integral exactly when  $f(x)$  is a polynomial of degree  $2N - 1$  or less. As we shall see below, the  $\{x_i\}$  are zeros of a polynomial  $p_N$  of degree  $N$  orthogonal (with respect to the weight function  $w(x)$ ) to the space of all lower-degree polynomials (see Eq. 11.96). Tables of points and weights for the classical orthogonal polynomials for different numbers of quadrature points are given by Abramowitz (1964), for example.

► **Exercise 11.7** The Lagrange interpolating polynomials are defined as

$$L_i(x) = \prod_{\substack{j=1 \\ j \neq i}}^N \frac{x - x_j}{x_i - x_j}. \quad (11.64)$$

- a. Show that  $L_i(x)$  is a polynomial of degree  $N - 1$ .
- b. Show that  $L_i(x)$  is equal to 1 at  $x = x_i$  and equal to 0 at the  $N - 1$  nodes  $x = x_j$ .
- c. Let  $f(x) = L_i(x)$  in Eq. 11.63. Show that

$$W_i = \int_a^b w(x) L_i(x) dx. \quad (11.65)$$

It turns out that there is a simple way to calculate the points and weights for integration by Gaussian quadrature for any common set of classical polynomials. What makes the procedure remarkable is not only the ease and accuracy of the algorithm, but also the conceptual bridge it establishes between integration by Gaussian quadrature and pseudospectral theory.

Consider a set of polynomials,  $\{p_n, n = 0, \dots, N - 1\}$ , satisfying the orthogonality relationship  $\int_a^b w(x) p_m(x) p_n(x) dx = \delta_{mn}$ . This is a set of orthogonality relations reminiscent of Eq. 11.35 but with the inner product defined with respect to the positive weight

function  $w(x)$ . If the points and weights are chosen according to an  $N$ -point Gaussian quadrature, Eq. 11.63 becomes an equality for polynomials up to degree  $2N - 1$ , and therefore

$$\int_a^b w(x) p_m(x) p_n(x) dx = \sum_{i=0}^{N-1} W_i p_m(x_i) p_n(x_i) = \delta_{mn}. \quad (11.66)$$

Defining the function

$$\phi_n(x) = \sqrt{w(x)} p_n(x), \quad (11.67)$$

and the corresponding matrix  $\Phi$  with elements

$$\Phi_{in} = \sqrt{W_i} p_n(x_i), \quad (11.68)$$

we can rewrite Eq. 11.66 as

$$\Phi^\dagger \Phi = \mathbf{1}, \quad (11.69)$$

indicating that  $\Phi$  is a unitary matrix. Note the complete correspondence between Eqs. 11.68 and 11.69 and Eqs. 11.37 and 11.39 if we identify  $\Delta_j^{1/2} \phi_n(x_j) = \sqrt{W_j} p_n(x_j)$  or

$$W_i = \Delta_i w(x_i). \quad (11.70)$$

Consider now the integral  $\int_a^b w(x) p_m(x) x p_n(x) dx$ . This is a polynomial of degree no higher than  $2N - 1$ , and so Gaussian quadrature must be exact:

$$\int_a^b w(x) p_m(x) x p_n(x) dx = \sum_{i=0}^{N-1} W_i p_m(x_i) x_i p_n(x_i) = \sum_{i,j=0}^{N-1} \Phi_{mi}^\dagger x_{ij} \Phi_{jn} = X_{mn} \quad (11.71)$$

or in matrix notation

$$\mathbf{X} = \Phi^\dagger \mathbf{x} \Phi, \quad (11.72)$$

where  $\mathbf{X}$  is an  $N \times N$  matrix with elements  $X_{mn}$  defined by the RHS of Eq. 11.71 and  $\mathbf{x}$  is a diagonal matrix with elements  $x_{ij}$ . The decomposition in Eq. 11.72 is unique (for a given ordering of the  $\{x_i\}$ ) and hence  $x_{ii}$  is the  $i$ th Gaussian quadrature node and  $\Phi_{in}$  must satisfy Eq. 11.68. Eq. 11.72 suggests the following simple procedure for finding Gaussian quadrature points and weights:

1. Construct the  $N \times N$  matrix representation of the  $\hat{x}$  operator,  $\mathbf{X}$ , using the first  $N$  basis functions:

$$X_{mn} = \int_a^b \phi_m(x) x \phi_n(x) dx = \int_a^b w(x) p_m(x) x p_n(x) dx. \quad (11.73)$$

The matrix  $\mathbf{X}$  is tridiagonal, a consequence of the three-term recursion relation satisfied by classical orthogonal polynomials. Examples of  $\mathbf{X}$  for several of the more common classical polynomials are given in Table 11.1.

2. Diagonalize  $\mathbf{X}$  by a unitary transformation:

$$\mathbf{U}^{-1} \mathbf{X} \mathbf{U} = \Phi \mathbf{X} \Phi^\dagger = \mathbf{x}. \quad (11.74)$$

**Table 11.1** Properties of the classical orthogonal polynomials and the matrix representation of  $\hat{x}$  in their basis

Chebyshev (2 <sup>nd</sup> kind)		Legendre
	$U_n(x); x \in [-1, 1]$	$P_n(x); x \in [-1, 1]$
$w(x)$	$(1 - x^2)^{1/2}$	1
$\mathbf{X}$	$\begin{pmatrix} & \frac{1}{2} & & \\ \frac{1}{2} & & \frac{1}{2} & \\ & \frac{1}{2} & & \ddots \\ & & \ddots & \ddots \end{pmatrix}$	$\begin{pmatrix} & \frac{1}{(1\cdot 3)^{1/2}} & & \\ \frac{1}{(1\cdot 3)^{1/2}} & & \frac{2}{(3\cdot 5)^{1/2}} & \\ & \frac{2}{(3\cdot 5)^{1/2}} & & \frac{3}{(5\cdot 7)^{1/2}} \\ & & \frac{3}{(5\cdot 7)^{1/2}} & \ddots \end{pmatrix}$
Laguerre		Hermite
	$L_n; x \in [0, \infty)$	$H_n(x); x \in (-\infty, \infty)$
$w(x)$	$e^{-x}$	$e^{-x^2}$
$\mathbf{X}$	$\begin{pmatrix} 1 & -1 & & & \\ -1 & 3 & -2 & & \\ & -2 & 5 & -3 & \\ & & -3 & 7 & \ddots \\ & & & & \ddots \end{pmatrix}$	$\begin{pmatrix} & \sqrt{\frac{1}{2}} & & \\ \sqrt{\frac{1}{2}} & & \sqrt{\frac{2}{2}} & \\ & \sqrt{\frac{2}{2}} & & \sqrt{\frac{3}{2}} \\ & & \sqrt{\frac{3}{2}} & \ddots \end{pmatrix}$

The eigenvalues  $\{x_i\}$  are the integration points of Eq. 11.71 and hence the Gaussian quadrature points of Eq. 11.63. The weights can be easily extracted from the first row of the transformation matrix,  $\mathbf{U} = \Phi^\dagger$  (first column of  $\Phi$ ). Since the lowest member of every set of classical polynomials is a constant, we have from Eq. 11.66 that  $p_0(x_i) = (\int_a^b w(x) dx)^{-1/2}$ . Substituting into Eq. 11.68 we obtain an explicit equation for the weights:

$$W_i = \Phi_{i0}^2 \int_a^b w(x) dx. \quad (11.75)$$

Quadrature points and weights for several of the more common classical polynomials are shown in Figure 11.3 for the case  $N = 12$ .

Historically, the procedure of constructing  $\mathbf{X}$  and diagonalizing was introduced by Harris, Engerholm and Gwinn (Harris, 1965; henceforth HEG) in the context of a novel procedure for calculating matrix elements of the form  $\int \phi_n(x) V(x) \phi_m(x) dx$  (Section 11.4). The relationship between their method and Gaussian quadrature was established later by Dickinson and Certain (Dickinson, 1968), who showed that the characteristic equation for the points and weights obtained by matrix diagonalization agrees with known expressions from Gaussian quadrature theory. Our discussion above represents an equally rigorous proof, bypassing the lengthy algebra of Dickinson and Certain by invoking the uniqueness of the decomposition Eq. 11.72. The relationship between diagonalizing  $\mathbf{X}$  and Gaussian

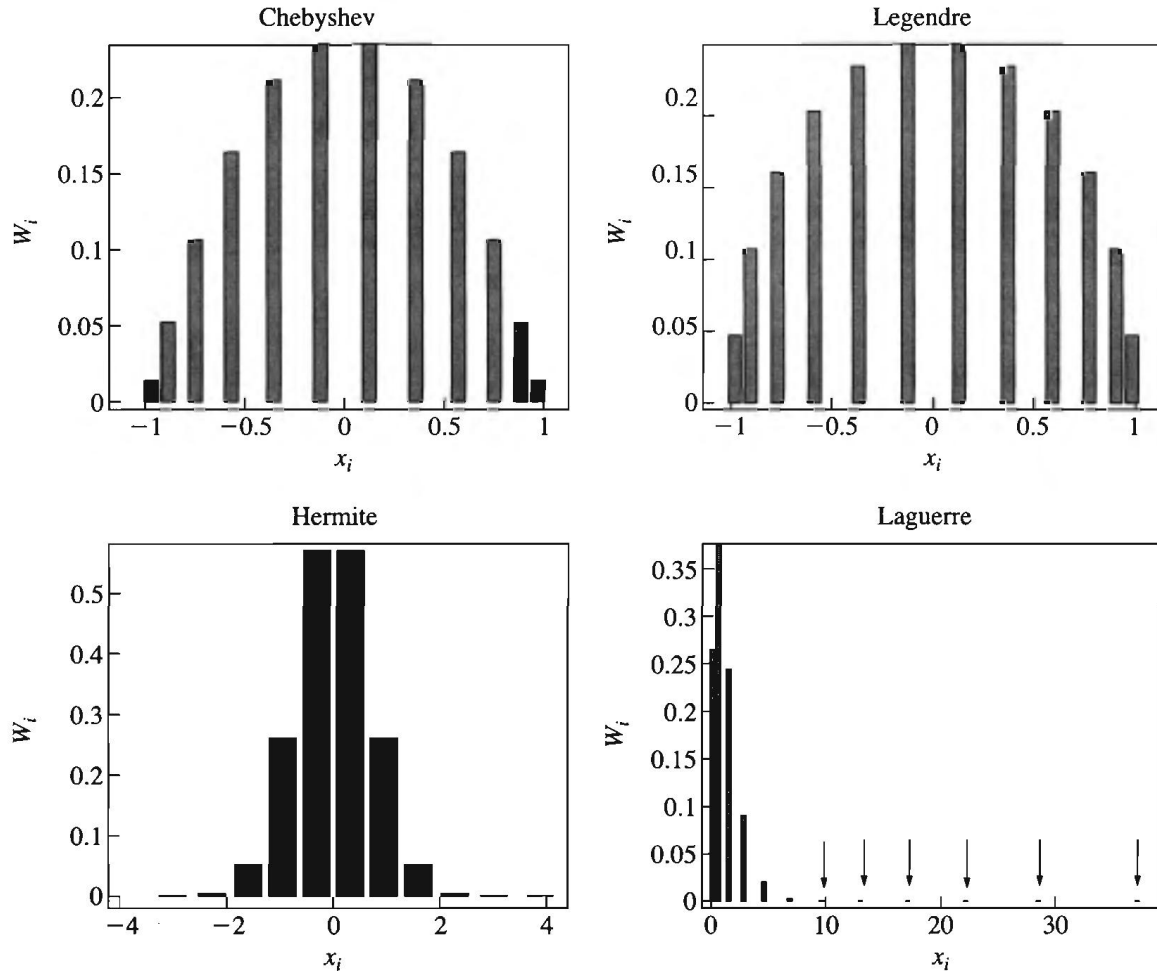


**Figure 11.3** Quadrature points and weights for several of the more common orthogonal polynomials. In all cases  $N = 12$ , although the smallest weights are not always visible.

quadrature was discovered independently in the applied mathematics community by Golub and Welsch (1969).

### 11.3.2 Properties of the Gaussian Quadrature Pseudospectral Functions

Having obtained an orthogonal collocation matrix in the previous section whose points and weights are based on Gaussian quadrature, in this section we explore the properties of the corresponding pseudospectral functions.

We begin by noting that from Eq. 11.74, the columns of  $\Phi^\dagger$  are the eigenvectors of  $\mathbf{X}$ , hence the *eigenfunctions* of  $\hat{x}_N$  are given by

$$\theta_i(x) = \sum_{n=1}^N \Phi_{ni}^\dagger \phi_n(x), \quad \text{with } \Phi_{ni}^\dagger = \langle \phi_n | \theta_i \rangle. \quad (11.76)$$

This is exactly Eq. 11.43 (and 11.46), and the  $\{\theta_i\}$  are the localized pseudospectral functions that are linear combinations of the delocalized spectral basis functions.

The explicit form of the Gaussian quadrature pseudospectral functions may be obtained by substituting Eqs. 11.67 and 11.68 into Eq. 11.41:

$$\theta_j(x) = \sum_{n=1}^N \phi_n(x) \Phi_n^*(x_j) = \sum_{n=1}^N w^{1/2}(x) p_n(x) W_j^{1/2} p_n(x_j). \quad (11.77)$$

Comparing this equation with the grid orthogonality relation

$$\sum_{n=1}^N W_i^{1/2} p_n(x_i) W_j^{1/2} p_n(x_j) = \delta_{ij} \quad (11.78)$$

we find that

$$\left( \frac{W_i}{w(x_i)} \right)^{1/2} \theta_j(x_i) = \delta_{ij}. \quad (11.79)$$

Using Eq. 11.77, we may conclude that the Gaussian quadrature pseudospectral functions are related in a simple way to the Lagrange interpolating polynomials (see Exercise 11.7) with nodes at the Gaussian quadrature points:

$$L_j(x) = \prod_{i \neq j=1}^N \frac{x - x_i}{x_j - x_i} = \left( \frac{W_j}{w(x)} \right)^{1/2} \theta_j(x). \quad (11.80)$$

This follows from the following observations. First, from Eq. 11.77 we see that  $\theta_j(x)/w^{1/2}(x)$  is a polynomial of degree  $N - 1$ . The nodes of this polynomial determine the polynomial uniquely up to an overall multiplicative factor. Substituting  $x = x_i$  in Eq. 11.80 we see that the LHS and the RHS have nodes at the same location. Finally, Eq. 11.79 guarantees that the overall scaling factor in Eq. 11.80 is the correct one. Figure 11.4 shows the (scaled) Legendre polynomials and the (scaled) associated pseudospectral functions, for the case  $N = 12$ .

It is useful to rewrite Eq. 11.73 in Dirac notation:

$$X_{mn} = \langle \phi_m | \hat{x} | \phi_n \rangle = \langle \phi_m | P_N \hat{x} P_N | \phi_n \rangle, \quad (11.81)$$

where we are allowed to introduce the orthogonal projection operator  $P_N$  on both sides of  $\hat{x}$  since both  $\phi_n$  and  $\phi_m$  are unaffected by this projection operator. For future use we define the operator

$$\hat{x}_N = P_N \hat{x} P_N. \quad (11.82)$$

The  $ij$ th element of Eq. 11.74 can now be rewritten as

$$\left( \Phi \mathbf{X} \Phi^\dagger \right)_{ij} = \sum_{m,n=1}^N \langle \theta_i | \phi_m \rangle \langle \phi_m | \hat{x}_N | \phi_n \rangle \langle \phi_n | \theta_j \rangle \quad (11.83)$$

$$= \langle \theta_i | \hat{x}_N | \theta_j \rangle = x_i \delta_{ij}, \quad (11.84)$$

showing in a basis independent representation that the localized pseudospectral functions are eigenfunctions of the projected  $\hat{x}$  operator,  $\hat{x}_N$ . In the coordinate representation the eigenvalue equation takes the form

$$\hat{x}_N \theta_i(x) = x_i \theta_i(x). \quad (11.85)$$

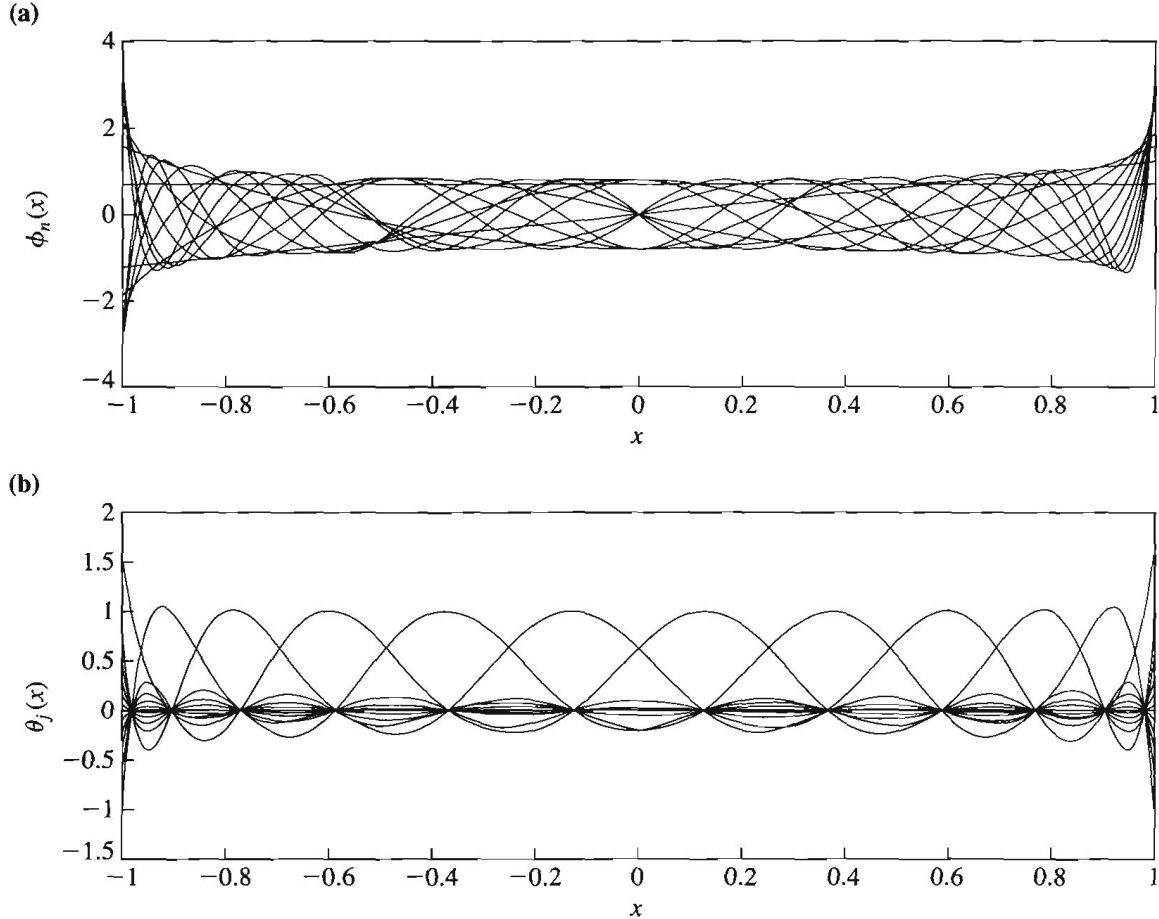


**Figure 11.4** (a) The first 12 (scaled) Legendre polynomials,  $\phi_n(x) = w^{1/2}(x)p_n(x)$ . (b) The 12 (scaled) DVR functions,  $L_j(x) = (W_j^{1/2}/w^{1/2}(x))\theta_j(x)$  (see text). The scaled DVR functions are identical to the Lagrange interpolating functions, and thus have the property that they are 1 at their own grid point and vanish at each other grid point.

### 11.3.3 Derivation of the Theory of Gaussian Quadrature from the Properties of the Pseudospectral Functions

In Section 11.3.1 we assumed the existence of Gaussian quadrature points and weights that give exact values for integrals up to degree  $2N - 1$ . We now show that we do not need to assume this; the theory of Gaussian quadrature can be derived from first principles from the properties of the pseudospectral basis functions.

We begin by returning to Eq. 11.73. Inserting two complete sets of the  $\{\theta_i\}$  we obtain

$$X_{mn} = \sum_{i,j=1}^N \langle \phi_m | \theta_i \rangle \langle \theta_i | \hat{x}_N | \theta_j \rangle \langle \theta_j | \phi_n \rangle = \sum_{i=1}^N \phi_m^*(x_i) x_i \phi_n(x_i) \Delta_i, \quad (11.86)$$

where we have used Eqs. 11.49, 11.37 and 11.84. Comparing with Eq. 11.73 and using Eq. 11.70 we see that

$$\int_a^b w(x) p_m(x) x p_n(x) dx = \sum_{i=0}^{N-1} W_i p_m(x_i) x_i p_n(x_i). \quad (11.87)$$

This is exactly the Gaussian quadrature relation that was *assumed* in Eq. 11.71. Here the exact equivalence between the integral and a weighted sum of specific values of the integrand is not assumed, but emerges automatically from the properties of the  $\{\theta_i\}$ .

We can use Eq. 11.84 to show that the Gaussian quadrature points and weights give an exact result for the integral of the form of Eq. 11.63 with  $f(x)$  *any* polynomial of degree  $2N - 1$  or lower; that is, we can use the properties of the  $\{\theta_i\}$  to prove the usual statement of Gaussian quadrature in Eq. 11.63 (Degani, 2005). Consider the integral

$$\int_a^b w(x) x^{n_1} x^{n_2} dx \quad 0 \leq n_1, n_2 \leq N - 1. \quad (11.88)$$

We define  $\bar{x}^n = w^{1/2}(x)x^n$ . Since both  $\bar{x}^{n_1}$  and  $\bar{x}^{n_2}$  lie within the space  $\mathcal{H}_N$  we can introduce the projection operator  $P_N$  before and after the central factor of  $x$  to obtain

$$\int_a^b \bar{x}^{n_1} x \bar{x}^{n_2} dx = \int_a^b w(x) x^{n_1} \hat{x}_N x^{n_2} dx \quad (11.89)$$

$$= \sum_{i,j=1}^N \langle \bar{x}^{n_1} | \theta_i \rangle \langle \theta_i | \hat{x}_N | \theta_j \rangle \langle \theta_j | \bar{x}^{n_2} \rangle \quad (11.90)$$

$$= \sum_i \Delta_i^{1/2} \bar{x}_i^{n_1} x_i \Delta_i^{1/2} \bar{x}_i^{n_2} = \sum_i W_i x_i^{n_1+n_2+1}, \quad (11.91)$$

where we have used Eqs. 11.56, 11.85 and 11.70. Equation 11.91 establishes that for any monomial  $f(x) = x^j$ ,  $j = 0, \dots, 2N - 1$ ,

$$\int_a^b w(x) f(x) dx = \sum_i W_i f(x_i). \quad (11.92)$$

By linearity, Eq. 11.92 holds for any *polynomial* up to degree  $2N - 1$ .

A well-known property of Gaussian quadrature points is that they fall on the zeros of the polynomial of degree  $N$  that is orthogonal to the space of the  $N$  lower polynomials of degree  $0, \dots, N - 1$ . This may be derived simply as follows (Degani, 2005). Consider

$$\langle \theta_i | \bar{x}^{N+1} \rangle = \langle \theta_i | \hat{x} | \bar{x}^N \rangle = \langle \theta_i | \hat{x}_N | \bar{x}^N \rangle = x_i \langle \theta_i | \bar{x}^N \rangle. \quad (11.93)$$

Continuing this procedure recursively we find that

$$\langle \theta_i | \bar{x}^{N+1} \rangle = W_i^{1/2} x_i^{N+1}, \quad (11.94)$$

where the factor  $W_i^{1/2}$  comes from the last factor

$$\langle \theta_i | \bar{1} \rangle = \int_a^b w^{1/2}(x) \theta_i(x) dx = W_i^{1/2} \quad (11.95)$$

(cf. Eqs. 11.56, 11.70). By linearity we have that  $\langle \theta_i | \bar{p} \rangle = W_i^{1/2} p(x_i)$  for  $w^{1/2} p(x)$  in  $\mathcal{H}_{N+1}$  (note that the result applies to  $N + 1$ , not just to  $N$ ). Now consider a polynomial  $p_\perp$  of degree  $N + 1$  that is orthogonal to the space  $\mathcal{H}_N$ . Then

$$0 = \langle \theta_i | \bar{p}_\perp \rangle = W_i^{1/2} p(x_i), \quad i = 1, \dots, N. \quad (11.96)$$

Thus, the polynomial of degree  $N + 1$  that is orthogonal to  $\mathcal{H}_N$  must vanish at the points  $\{x_i\}$ ,  $i = 1, \dots, N$ , and conversely, the  $N$  quadrature points must fall at the zeros of the polynomial  $p_\perp$  that is of degree  $N + 1$  and orthogonal to  $\mathcal{H}_N$ .

- **Exercise 11.8** Show that Eq. 11.95

$$\langle \theta_i | \bar{l} \rangle = \int_a^b w^{1/2}(x) \theta_i(x) dx = W_i^{1/2} \quad (11.97)$$

is consistent with Eqs. 11.80 and 11.65.

## 11.4 Representation of the Hamiltonian in the Reduced Space

In the previous sections we introduced the notions of spectral projection, collocation and the pseudospectral basis. The key results were as follows:

1. Spectral projection and collocation are generally defined by two distinct projection operators.
2. Spectral projection can be represented in either a delocalized spectral basis or a localized pseudospectral basis. These two representations of the spectral projection operator are completely equivalent as long as the transformation between the spectral and pseudospectral basis is unitary (orthogonal):

$$P_N = \sum_{n=1}^N |\phi_n\rangle\langle\phi_n| = \sum_{i=1}^N |\theta_i\rangle\langle\theta_i|. \quad (11.98)$$

3. The projection operator for collocation is conveniently represented in the pseudospectral basis as

$$P_N = \sum_{i=1}^N |\theta_i\rangle\langle x_i|. \quad (11.99)$$

Until now we have focused primarily on the action of these projectors on wavefunctions. We now turn to the construction of the Hamiltonian operator  $H = T(\hat{p}) + V(\hat{x})$  using these projectors. In this section we will discuss construction of the Hamiltonian in the spectral basis,  $P_N = \sum_{n=1}^N |\phi_n\rangle\langle\phi_n|$ . In the following two sections we will discuss construction of the Hamiltonian under orthogonal projection in a pseudospectral basis,  $P_N = \sum_{i=1}^N |\theta_i\rangle\langle\theta_i|$ . When this is done using pseudospectral functions derived from classical polynomials the method is known as the Discrete Variable Representation (Section 11.5). When the pseudospectral functions are based on complex exponentials it is known as the Fourier method (Section 11.6). The collocation projector  $P_N = \sum_{i=1}^N |\theta_i\rangle\langle x_i|$  will appear at various points in our discussion.

Our treatment here will be cast in terms of one-dimensional systems. One can construct a multidimensional extension in a straightforward way using the direct product. Consider a Hamiltonian in two dimensions,

$$H = T_x + T_y + V(x, y), \quad (11.100)$$

and a finite basis representation that is of direct product form,

$$|\Phi_{mn}\rangle = |\phi_m^x\rangle \otimes |\phi_n^y\rangle, \quad (11.101)$$

where  $\otimes$  is the tensor product. The Hamiltonian matrix in multidimensions takes the form

$$\langle \Phi_{m'n'} | H | \Phi_{mn} \rangle = \langle \phi_{m'}^x | \otimes \langle \phi_{n'}^y | T_x + T_y + V(x, y) | \phi_m^x \rangle \otimes \phi_n^y \rangle \quad (11.102)$$

$$\begin{aligned} &= \langle \phi_{m'}^x | T_x | \phi_m^x \rangle \otimes \delta_{nn'}^y + \delta_{mm'}^x \otimes \langle \phi_{n'}^y | T_y | \phi_n^y \rangle \\ &\quad + \langle \phi_{m'}^x | \otimes \langle \phi_{n'}^y | V(x, y) | \phi_m^x \rangle \otimes \phi_n^y \rangle. \end{aligned} \quad (11.103)$$

The size of the direct product basis grows exponentially with the number of degrees of freedom, and becomes prohibitively large at 5–10 degrees of freedom. In the pseudospectral basis, one can similarly build a representation of the Hamiltonian in direct product form. Defining

$$|\Theta_{ij}\rangle = |\theta_i^x\rangle \otimes |\theta_j^y\rangle \quad (11.104)$$

we can write the Hamiltonian matrix in multidimensions as

$$\langle \Theta_{i'j'} | H | \Theta_{ij} \rangle = \langle \theta_{i'}^x | T_x | \theta_i^x \rangle \otimes \delta_{jj'}^y + \delta_{ii'}^x \otimes \langle \theta_{j'}^y | T_y | \theta_j^y \rangle + \langle \theta_{i'}^x | \otimes \langle \theta_{j'}^y | V(x, y) | \theta_i^x \rangle \otimes \theta_j^y \rangle. \quad (11.105)$$

However, one of the great attractions of the use of a pseudospectral basis is the possibility of avoiding the direct product form of Eq. 11.105. This is a subject of considerable current interest (Littlejohn, 2002; Dawes, 2004; Degani, 2005).

### 11.4.1 Spectral Projection of the Hamiltonian

Consider a Hamiltonian that consists of a sum of kinetic and potential energy operators:

$$H = \hat{p}^2/2m + V(\hat{x}) = T(\hat{p}) + V(\hat{x}). \quad (11.106)$$

If one applies spectral projection down to an  $N$ -dimensional Hilbert space the truncated operators can be written as

$$H_N = P_N T(\hat{p}) P_N + P_N V(\hat{x}) P_N, \quad (11.107)$$

where

$$P_N = \sum_{n=1}^N |\phi_n\rangle \langle \phi_n|. \quad (11.108)$$

Inserting Eq. 11.108 into Eq. 11.107 we see that the necessary matrix elements are of the form

$$\langle \phi_n | T(\hat{p}) | \phi_m \rangle \quad \text{and} \quad \langle \phi_n | V(\hat{x}) | \phi_m \rangle. \quad (11.109)$$

(The index  $m$  should not be confused with the mass, the latter appearing only in the combination  $\frac{1}{2m}$ .) While the kinetic energy operator can actually become very complicated in multidimensions, in one dimension the  $T$  operator is generally quite simple. As a result, in one dimension the matrix elements in the spectral representation,  $T_{mn} = \langle \phi_m | T | \phi_n \rangle$ , can generally be written down analytically. For example, if  $T = \hat{p}^2/2m$ , then

$$T_{mn} = \langle \phi_m | T | \phi_n \rangle = -\frac{\hbar^2}{2m} \int_a^b \phi_m^*(x) \frac{\partial^2}{\partial x^2} \phi_n(x) dx \quad (11.110)$$

for which there are generally analytic expressions. The potential energy matrix elements

$$V_{mn} = \langle \phi_m | V(\hat{x}) | \phi_n \rangle = \int_a^b \phi_m^*(x) V(x) \phi_n(x) dx \quad (11.111)$$

generally are not known analytically in the spectral representation. However, one may employ Gaussian quadrature to approximate the integral of a function  $f(x)$  by a finite sum:

$$\int_a^b w(x) f(x) dx \approx \sum_{i=1}^N W_i f(x_i). \quad (11.112)$$

Using the expression  $\phi_l(x) = w^{1/2}(x) p_l(x)$ ,  $l = n, m$ , we make the identification  $f(x) = p_n(x) V(x) p_m(x)$  in the quadrature formula and obtain the following approximate expression for the individual matrix elements:

$$V_{mn} \approx \sum_{i=1}^n W_i p_m(x_i) V(x_i) p_n(x_i), \quad (11.113)$$

with the points and weights taken from the theory of Gaussian quadrature.

#### 11.4.2 The HEG Algorithm

In constructing the different matrix elements of  $V$ , one would a priori use different numbers and locations of quadrature points to calculate each of the different matrix elements. However, the procedure developed by HEG (Section 11.3.1) allows one to calculate all the  $N \times N$  potential energy matrix elements at once, using the same quadrature points for all integrals. The HEG procedure for calculating potential energy matrix elements is as follows (Harris, 1965):

1. Construct the  $N \times N$  matrix representation of the  $\hat{x}$  operator,  $\mathbf{X}_N$ , using the first  $N$  basis functions. This matrix has elements

$$X_{mn} = \int_a^b \phi_m(x) x \phi_n(x) dx = \int_a^b w(x) p_m(x) x p_n(x) dx. \quad (11.114)$$

The matrix  $\mathbf{X}_N$  is tridiagonal, a consequence of the form of the three-term recursion relation satisfied by most classical orthogonal polynomials.

2. Diagonalize  $\mathbf{X}_N$  by a unitary transformation:

$$\mathbf{U}_N^\dagger \mathbf{X}_N \mathbf{U}_N = \mathbf{x}, \quad (11.115)$$

where  $\mathbf{x}_{ij} = x_i \delta_{ij}$ . These first two steps in the HEG procedure are identical to the procedure described in Section 11.3.1 to calculate Gaussian quadrature points and weights by matrix diagonalization.

3. Compute  $V(\mathbf{x})$ . Since  $\mathbf{x}$  is diagonal,  $(V(\mathbf{x}))_{ij} = V(x_i)\delta_{ij}$ .
4. Transform back to the basis of orthogonal polynomials:

$$\mathbf{V}_N^{\text{HEG}} = \mathbf{U}_N V(\mathbf{x}) \mathbf{U}_N^\dagger. \quad (11.116)$$

Multiplying out the matrices in Eq. 11.116 and using Eq. 11.68 we obtain

$$(\mathbf{V}_N^{\text{HEG}})_{mn} = \sum_{i=1}^n \mathbf{U}_{mi} V(x_{ii}) (\mathbf{U}^\dagger)_{in} = \sum_{i=1}^n W_i p_m(x_i) V(x_i) p_n(x_i). \quad (11.117)$$

Equation 11.117 is identical with Eq. 11.113, the expression obtained with an  $N$ -point Gaussian quadrature approximation to the integral  $(\mathbf{V}_N(\hat{x}))_{mn}$ , if the  $\{x_i\}$  are identified with the Gaussian quadrature points and the  $\{W_i\}$  are identified with the Gaussian weights (see Section 11.3.1).

An alternative perspective on the approximation inherent in the HEG method is obtained by noting that

$$\mathbf{V}_N^{\text{HEG}} = \mathbf{U}_N V(\mathbf{x}) \mathbf{U}_N^\dagger = V(\mathbf{X}_N). \quad (11.118)$$

The proof is straightforward. From Eq. 11.115 we have  $\mathbf{U}_N^\dagger \mathbf{X}_N \mathbf{U}_N = \mathbf{x}$ , and therefore

$$\mathbf{U}_N^\dagger \mathbf{X}_N^n \mathbf{U}_N = (\mathbf{U}_N^\dagger \mathbf{X}_N \mathbf{U}_N)^n = \mathbf{x}^n. \quad (11.119)$$

Since Eq. 11.119 holds for all powers  $n$ , it is easily seen to hold for polynomial  $V(x)$ :

$$\mathbf{U}_N^\dagger V(\mathbf{X}_N) \mathbf{U}_N = V(\mathbf{x}), \quad (11.120)$$

which is equivalent to Eq. 11.118. Thus, the key approximation in the HEG method can be expressed as the replacement

$$\mathbf{V}_N \rightarrow V(\mathbf{X}_N). \quad (11.121)$$

The matrices with subscript  $N$  are all defined here in a particular basis, namely that of the orthogonal functions. However, the approximation inherent in the HEG method can also be expressed in a basis-independent fashion. Formally, the matrix  $\mathbf{X}_N$  corresponds to the operator

$$\hat{x}_N = P_N \hat{x} P_N \quad (11.122)$$

(cf. Eq. 11.82). Comparing Eq. 11.124 with Eq. 11.107, and using Eqs. 11.118 and 11.122, we see that the essential approximation in the HEG method may be expressed more abstractly as the replacement

$$V_N(\hat{x}) = P_N V(\hat{x}) P_N \rightarrow V(\hat{x}_N) = V(P_N \hat{x} P_N), \quad (11.123)$$

where we now have a basis-independent representation for the approximation. The advantage to this basis-independent representation is that it indicates that the approximation is independent of the basis, and hence the numerical results should be identical whether calculated in a spectral basis as in the HEG method or in a pseudospectral basis as in the DVR method described below. Moreover, if the order of approximation can be quantified in one basis we know what it must be in the other basis as well.

This completes the calculation of the matrix elements  $V_{nm}$ . These matrix elements can then be used to compute eigenvalues and eigenfunctions of the full Hamiltonian as follows (Harris, 1965):

5. Construct the approximate Hamiltonian matrix by adding the kinetic and potential contributions:

$$\mathbf{H}_N^{\text{HEG}} \equiv \mathbf{T}_N + \mathbf{V}_N^{\text{HEG}}. \quad (11.124)$$

6. Diagonalize the matrix  $\mathbf{H}_N^{\text{HEG}}$  to solve the TISE, or to propagate the TDSE according to Eq. 11.10 or 11.11.

## 11.5 The Discrete Variable Representation

The Discrete Variable Representation or DVR method is a pseudospectral method for calculating matrix elements of the Hamiltonian (Light, 1985). What is specific to the DVR method is that the pseudospectral basis is related to the original spectral basis by an orthogonal collocation matrix based on Gaussian quadrature points and weights. Since many of the properties of the DVR method are common to all pseudospectral methods we begin by presenting the elements of the DVR method within the more general context of the evaluation of the Hamiltonian in a pseudospectral basis. In Section 11.5.2 we present the specifics of the DVR algorithm, with some further discussion of its inherent assumptions and approximations.

### 11.5.1 Evaluation of the Hamiltonian in a Pseudospectral Basis

As in Section 11.4.1 we consider a Hamiltonian of the form  $H = T(\hat{p}) + V(\hat{x})$ . We seek an orthogonal projection onto  $\mathcal{H}_N$ , however now, instead of expressing the projector in terms of the spectral basis we use the pseudospectral form

$$P_N = \sum_{i=1}^N |\theta_i\rangle\langle\theta_i|. \quad (11.125)$$

Considering  $H_N = P_N T(\hat{p}) P_N + P_N V(\hat{x}) P_N$  in the pseudospectral basis it is clear that the necessary matrix elements are of the form

$$\langle\theta_i|T(\hat{p})|\theta_j\rangle \quad \text{and} \quad \langle\theta_i|V(\hat{x})|\theta_j\rangle. \quad (11.126)$$

In Section 11.4.1 we dismissed the kinetic energy terms very quickly but gave a lengthy discussion of the evaluation of the potential energy by Gaussian quadrature. Here the situation is to some extent reversed. In the pseudospectral basis, the evaluation of the potential energy matrix elements is given by a simple prescription. Since the basis functions  $\{\theta_i\}$  are localized and satisfy the orthonormality relation  $\langle\theta_i|\theta_j\rangle = \delta_{ij}$  it seems plausible to make the replacement

$$V_{ij} = \langle\theta_i|V(\hat{x})|\theta_j\rangle \rightarrow V(x_i)\delta_{ij}. \quad (11.127)$$

The replacement in Eq. 11.127 is the key step in all pseudospectral methods. In particular, it is the central approximation of the DVR method described in this section as well as in the Fourier method, described in Section 11.6.

For the DVR method it turns out that the replacement in Eq. 11.127 represents an approximation identical to the Gaussian quadrature approximation in the HEG method. We will express this approximation explicitly in terms of Gaussian quadrature at the end of Section 11.5.2, after we have presented the DVR algorithm. However, we can already see that the approximation is identical to that of HEG by the following consideration. Since in the DVR method the orthogonal collocation matrix is based on Gaussian quadrature points and weights, the pseudospectral basis functions satisfy the equation  $\hat{x}_N|\theta_i\rangle = x_i|\theta_i\rangle$  (cf. Eq. 11.85). Combining this relation with our earlier result that the central approximation in the HEG method can be written as  $P_N V(\hat{x}) P_N \rightarrow V(P_N \hat{x} P_N) = V(\hat{x}_N)$  (Eq. 11.123) and using the pseudospectral form for the projector (Eq. 11.125), the DVR pseudospectral matrix elements take the form

$$V(\hat{x}_N)_{ij} = \sum_{k,l=1}^N \langle \theta_i | V(|\theta_k\rangle \langle \theta_k| \hat{x} |\theta_l\rangle \langle \theta_l|) | \theta_j \rangle \quad (11.128)$$

$$= \sum_{k=1}^N \langle \theta_i | V(|\theta_k\rangle x_k \langle \theta_k|) | \theta_j \rangle \quad (11.129)$$

$$= \sum_{k=1}^N \langle \theta_i | \theta_k \rangle V(x_k) \langle \theta_k | \theta_j \rangle = V(x_i) \delta_{ij}. \quad (11.130)$$

It is interesting to note that one may give a different interpretation to the replacement in Eq. 11.127. If  $P_N$  is taken to be the nonorthogonal projector associated with collocation,  $P_N = \sum_{i=1}^N |\theta_i\rangle \langle x_i|$ , then

$$P_N \hat{x} P_N^\dagger = \sum_{i,j=1}^N |\theta_i\rangle \langle x_i| V(\hat{x}) |x_j\rangle \langle \theta_j| = \sum_{i=1}^N |\theta_i\rangle V(x_i) \langle \theta_i| \quad (11.131)$$

with no approximation. Does it make any difference which of these two interpretations is adopted? Possibly yes, in that it could lead to different prescriptions for how the projector for the kinetic energy should be chosen. Suppose that the kinetic energy operator is different depending on whether it is evaluated under spectral projection or under collocation projection, and suppose that its representation can be evaluated exactly for both projectors. It could potentially be preferable to use collocation projection, which is nonorthogonal but according to which the potential energy matrix elements have been evaluated exactly, rather than spectral projection, which is orthogonal, but according to which the potential energy matrix elements are only approximate. These remarks are highly speculative at this point, but the concept is interesting and may be worth pursuing.

We now turn to the calculation of the kinetic energy matrix in a pseudospectral basis. The calculation of these matrix elements is more complicated in the pseudospectral than in the spectral basis, but is not particularly difficult. It requires the calculation of second derivative matrix elements  $T_{ij}$  between two localized basis functions associated with dif-

ferent grid points  $i$  and  $j$ . Although at first glance this seems complicated, there is a quite simple procedure:

$$(\mathbf{T}^\theta)_{ij} = \langle \theta_i | T | \theta_j \rangle \quad (11.132)$$

$$= \sum_{n,m=1}^N \langle \theta_i | \phi_n \rangle \langle \phi_n | T | \phi_m \rangle \langle \phi_m | \theta_j \rangle \quad (11.133)$$

$$= \sum_{n,m=1}^N \Phi_{in} (\mathbf{T}^\phi)_{nm} \Phi_{mj}^\dagger \quad (11.134)$$

$$= (\Phi \mathbf{T}^\phi \Phi^\dagger)_{ij}, \quad (11.135)$$

where we have used Eqs. 11.46 and 11.47. Equation 11.135 expresses the second derivative matrix between pseudospectral basis functions,  $\mathbf{T}^\theta$ , in terms of a unitary transformation on the second derivative matrix in the spectral basis  $\mathbf{T}^\phi$ . Once the transformation  $\Phi$  between the spectral and the pseudospectral basis is known,  $\mathbf{T}^\theta$  is readily calculated.

A different perspective is obtained by rewriting Eq. 11.132 in the following form:

$$(\mathbf{T}^\theta)_{ij} = \sum_{n=1}^N \langle \theta_i | \phi_n \rangle \langle \phi_n | T | \theta_j \rangle \quad (11.136)$$

$$\approx -\frac{\hbar^2}{2m} \sum_{n=1}^N \phi_n(x_i) \left. \frac{\partial^2 \phi_n}{\partial x^2} \right|_{x_j}. \quad (11.137)$$

Equation 11.137 gives an approximate route to calculating the second derivative matrix between two pseudospectral functions. The second derivative of the function  $\theta_j$  is evaluated at grid point  $j$  by representing the value at the grid point as a sum over a basis of orthogonal functions, and calculating (analytically) the second derivative of the basis functions at the grid point. The approximation comes from the fact that

$$\langle \theta_j | T | \phi_n \rangle \approx \langle x_j | T | \phi_n \rangle. \quad (11.138)$$

Equation 11.137, which calculates derivatives by means of a spectral method, has “global” accuracy, as opposed to the “local” accuracy of derivatives calculated by finite differencing methods. Global methods converge exponentially with the number of basis functions, while local methods converge polynomially. In particular, local methods for calculating derivatives can make significant errors in the high  $k$  components of the wavefunction, as shown in Figure 11.5. The nonlocal evaluation of the derivative operators is consistent with the uncertainty principle: since the evaluation of the coordinate operation is local it is natural that the evaluation of the momentum operation be nonlocal, when represented on a coordinate space grid.

### 11.5.2 The DVR Algorithm

To implement the DVR method the first two steps are exactly as in the method of HEG. However, in the third step the unitary transformation is performed on the *kinetic* energy

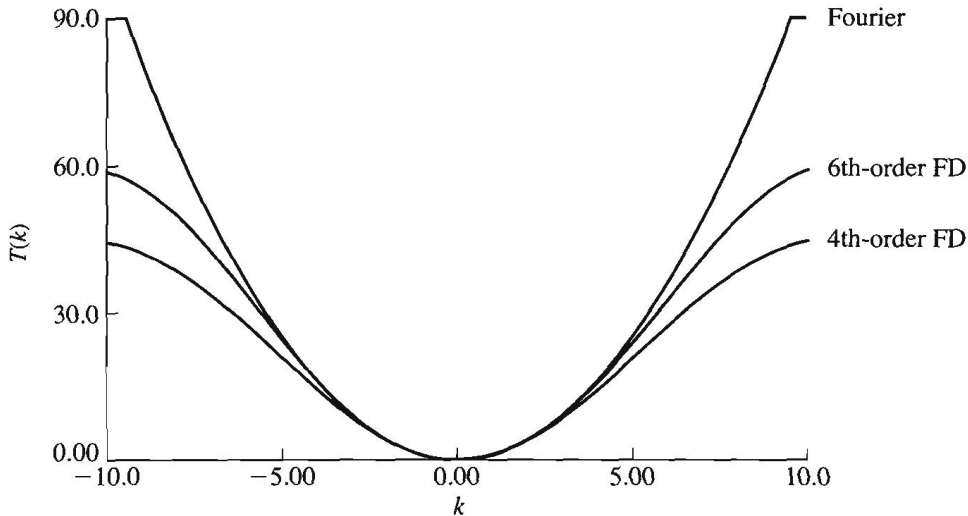


**Figure 11.5** Comparison of the kinetic energy operator spectrum for a spectral (Fourier) method with the fourth- and sixth-order finite difference methods. The spectral method, which is global, converges exponentially while finite difference methods, which are local, converge polynomially. Adapted from Kosloff (1993).

matrix instead of the potential energy matrix to leave the Hamiltonian in the pointwise representation. The procedure is as follows:

1. Construct the matrix representation of  $\hat{x}$  in a truncated basis of  $N$  orthogonal polynomials,  $\mathbf{x}_N$ . This matrix is tridiagonal; the form of the matrix elements for some common orthogonal polynomials are given in Table 11.1.
2. Diagonalize  $\mathbf{X}_N$  by a unitary transformation

$$\mathbf{U}^\dagger \mathbf{X}_N \mathbf{U} = \mathbf{x}, \quad (11.139)$$

where  $(\mathbf{x})_{ij} = x_i \delta_{ij}$ .

3. Compute  $V(\mathbf{x})$ . Since  $\mathbf{x}$  is diagonal,  $(V(\mathbf{x}))_{ij} = V(x_i) \delta_{ij}$ . It is this diagonal form of the potential energy matrix, and its construction by simple evaluation of  $V(x)$  at the grid points, that leads to both the attraction of the DVR method and its close kinship to the Fourier method described in the next section.
4. Calculate the kinetic energy matrix in the basis of orthogonal polynomials, which we denote  $\mathbf{T}_N^\phi$ . The matrix elements are normally known analytically and this matrix is typically diagonal or tridiagonal. In order that the Hamiltonian  $\mathbf{H}_N = \mathbf{T}_N + \mathbf{V}_N$  be expressed completely in the pseudospectral basis,  $\mathbf{T}_N^\phi$  must now be transformed by the same transformation  $\mathbf{U}$  that was used to transform the matrix  $\mathbf{V}_N$  to the pseudospectral basis:

$$\mathbf{T}_{ij}^{\text{DVR}} = (\mathbf{U}^\dagger \mathbf{T}^\phi \mathbf{U})_{ij}. \quad (11.140)$$

Note that this expression matches the general structure of Eq. 11.135.

5. Construct the DVR Hamiltonian by adding the kinetic and potential energies:

$$\mathbf{H}_N^{\text{DVR}} = \mathbf{T}_N^{\text{DVR}} + \mathbf{V}_N^{\text{DVR}} \quad (11.141)$$

6. Diagonalize the DVR Hamiltonian,  $\mathbf{H}_N^{\text{DVR}}$ .

From the DVR algorithm it is clear that the pseudospectral matrix  $\mathbf{H}_N^{\text{DVR}}$  differs from the spectral matrix  $\mathbf{H}_N^{\text{HEG}}$  of the previous section only in the choice of representation. Whereas the HEG constructs the orthogonal projection of the Hamiltonian onto  $\mathcal{H}_N$  using the spectral basis  $\{\phi_i\}$ , the DVR method constructs the Hamiltonian in the pseudospectral basis  $\{\theta_i\}$ . As discussed above, the two bases are related by an orthogonal (or unitary) transformation and thus

$$\mathbf{U} \mathbf{H}_N^{\text{DVR}} \mathbf{U}^\dagger = \mathbf{H}_N^{\text{HEG}}. \quad (11.142)$$

Since the Hamiltonians differ only by a unitary transformation, they must have identical eigenvalues and if used to propagate an initial wavefunction will give identical dynamics. This is consistent with what we have already seen at Eq. 11.123, that in a basis-independent formulation both algorithms make the replacement  $P_N V(\hat{x}) P_N \rightarrow V(P_N \hat{x} P_N)$ .

It follows that the DVR method contains the same approximation of  $N$ -point Gaussian quadrature integration as does the HEG method. From the discussion at Eq. 11.123 we can conclude that the pseudospectral matrix elements of the potential in the DVR method will be evaluated exactly, that is,

$$\langle \theta_i | V(\hat{x}) | \theta_j \rangle = \int \theta_i(x) V(x) \theta_j(x) dx = \sum_{k=1}^N W_k \theta_i(x_k) V(x_k) \theta_j(x_k) = V(x_i) \delta_{ij}, \quad (11.143)$$

provided that  $\theta_i(x) V(x) \theta_j(x) = w(x) f(x)$  with  $f(x)$  a polynomial of degree  $2N - 1$  or less. In summary, the replacement in Eq. 11.127 is an approximation to the evaluation of  $P_N H P_N$  at an accuracy equivalent to an  $N$ -point Gaussian quadrature approximation to the integral.

## 11.6 The Fourier Method

The Fourier method (Kosloff, 1983, 1988, 1993; Feit, 1982; Colbert, 1992; Willner, 2001) is a special case of a pseudospectral method on a grid of evenly spaced points. As in any pseudospectral method, the potential energy matrix is diagonal and is just given by the value of the potential at the grid point. The Fourier method has two implementations: the Fourier Grid Hamiltonian method, which involves construction of the Hamiltonian matrix in a pseudospectral Fourier basis (Section 11.6.4), and the Dynamic Fourier Method, in which the construction of matrices is avoided by calculating their action on the wavefunction directly via Fast Fourier Transform procedure (Section 11.6.5).

### 11.6.1 The Spectral Projector in the Fourier Method

In the Fourier method, the orthogonal basis functions are of the general form

$$\phi_k(x) \propto e^{ikx}. \quad (11.144)$$

The projector in the Fourier method depends on the choice of the range of  $x$  and  $k$ , but there is some residual freedom in the projector that depends on the exact choice of functions  $\{k\}$ . We will discuss here two choices, a continuous basis in  $k$  and a discrete basis in  $k$ .

### Continuous $k$ -Basis

It is ubiquitous in the literature on the Fourier method to restrict the Hilbert space to  $-K \leq k \leq K$ . Functions that have no components of  $|k|$  (or whose  $k$  components decay exponentially) beyond  $K$  are called “band-limited.” If the coordinate space range is infinite, then the ( $k$ -normalized) basis functions of the form in Eq. 11.144 are

$$\phi_k(x) = \frac{e^{ikx}}{\sqrt{2\pi}}, \quad -K \leq k \leq K, \quad -\infty < x < \infty. \quad (11.145)$$

The basis set corresponding to continuous values of  $k$ , Eq. 11.145, defines a projector operator that we denote  $P_{\square}$ :

$$P_{\square}(\hat{p}) = \int_{-K}^K |\phi_k\rangle \langle \phi_k| dk, \quad (11.146)$$

where the symbol  $\square$  is meant to suggest visually the band-limited range of  $k$ .

### Discrete $k$ -Basis

If one assumes that the Hilbert space spans only a finite range of coordinate space,  $0 \leq x \leq L$ , the Hilbert space is said to have “finite support.” We may define a projection operator associated with this finite range,

$$P_{\square}(\hat{x}) = \int_0^L |x\rangle \langle x| dx. \quad (11.147)$$

The normalized basis functions of the form in Eq. 11.144 are then determined by the condition

$$\int_0^L \phi_k^*(x) \phi_{k'}(x) dx = \delta_{kk'} = \frac{1}{L} \int_0^L e^{-ikx} e^{ik'x} dx. \quad (11.148)$$

Note that Eq. 11.148 can be satisfied only for discrete values of  $k$ , satisfying  $k - k' = \frac{n2\pi}{L}$  or

$$\Delta k = \frac{2\pi}{L}, \quad (11.149)$$

where  $\Delta k$  is the difference in  $k$  between two neighboring basis functions. Thus, the normalized basis functions are given by

$$\phi_k(x) = \frac{e^{ikx}}{\sqrt{L}} \quad 0 \leq x \leq L, \quad k = \kappa \Delta k, \quad -\infty < \kappa < \infty. \quad (11.150)$$

The restriction to discrete values of  $k$  corresponds to a projection operator  $P_{\square}(\hat{p})$  defined by the equation

$$P_{\square}(p) = \sum_{\kappa=-\infty}^{\infty} |p_{\kappa}\rangle \langle p_{\kappa}|, \quad (11.151)$$

where  $p_\kappa = \hbar\kappa \Delta k$ . The symbol  $\sqcup$  is meant to suggest visually the discrete, picket-fence-like structure of the projector in  $k$ . From the theory of Fourier series we know that the basis defined by Eq. 11.150 is complete with respect to the expansion of any periodic function with period  $L = 2\pi/\Delta k$  (see Section 6.2.3). Note that  $P_{\sqcup}(p)$  is close to but not identical to  $P_{\sqcap}(x)$ . Applying the former to a function  $\Psi(x)$  produces the same function as the latter on the domain  $0 \leq x \leq L$ , but produces in addition an infinite, periodically repeating series of replicas. Despite the fact that the two projectors are not identical, the functions they return have the same information content: from the periodic function one can construct the function on the interval  $[0, L]$ , and from the function on the interval  $[0, L]$  one can construct the periodic function. This is essentially the content of the Nyquist theorem, which states that for a function of finite support on  $[0, L]$ , there is no loss of information by sampling it at discrete values of  $k$  with  $\Delta k = 2\pi/L$ .

### The Combined $k$ -Basis

Can we combine the restriction of finite support on  $0 \leq x \leq L$  with the restriction of band limit,  $-K \leq k \leq K$ ? Strictly speaking, no: since  $P_{\sqcap}(\hat{x})$  and  $P_{\sqcup}(\hat{p})$  do not commute (because  $\hat{x}$  and  $\hat{p}$  do not), the product of the two is not Hermitian and therefore cannot be a projector. Note, however, that the close relative of  $P_{\sqcap}(\hat{x})$ ,  $P_{\sqcup}(\hat{p})$ , does commute with  $P_{\sqcap}(\hat{p})$  since they are both functions of  $\hat{p}$ . This combined projector can be written as

$$P = P_{\sqcap}(\hat{p})P_{\sqcup}(\hat{p}), \quad (11.152)$$

where here and henceforth we assume that  $2K/\Delta k = KL/\pi = N$ , where  $N$  is an integer (if this condition is not satisfied it is always possible to increase the value of  $K$  slightly). The combined projector has a simple geometrical interpretation in  $k$ -space: the operator  $P_{\sqcap}(\hat{p})$  corresponds to multiplication of a function in  $k$ -space by a rectangular envelope, while the operator  $P_{\sqcup}(\hat{p})$  corresponds to multiplication of a function in  $k$ -space by a picket fence. Clearly the order of these multiplications is immaterial and hence the operators commute.

The combined projection operator, Eq. 11.152, corresponds to a normalized basis  $\{\phi_\kappa\}$ ,

$$P = P_{\sqcap}(\hat{p})P_{\sqcup}(\hat{p}) = \sum_{\kappa=1}^N |\phi_\kappa\rangle\langle\phi_\kappa|, \quad (11.153)$$

where

$$\phi_\kappa(x) = \frac{e^{ik\Delta k x}}{\sqrt{L}} = \frac{e^{i2\pi\kappa x/L}}{\sqrt{L}}, \quad -\frac{N}{2} + 1 \leq \kappa \leq \frac{N}{2}, \quad -\infty < x < \infty. \quad (11.154)$$

Although strictly speaking the basis functions in Eq. 11.154 are defined over the domain  $-\infty < x < \infty$ , from the periodic function on the infinite domain one can trivially recover the function on the unit domain  $[0, L]$ .

### 11.6.2 The Orthogonal Collocation Matrix in the Fourier Method

There are two Fourier pseudospectral schemes, corresponding to the two different choices of  $k$ -basis (discrete and continuous) described in the previous section. We begin with the discrete basis defined by Eq. 11.154, and then turn to the continuous basis defined by Eq. 11.145.

### Discrete $k$ -Basis

In the discrete basis, the pseudospectral matrix is chosen to make the orthogonality relation exact:

$$\int_0^L \phi_{\kappa'}^*(x) \phi_{\kappa}(x) dx = \delta_{\kappa\kappa'} = \sum_{j=1}^N \phi_{\kappa'}^*(x_j) \phi_{\kappa}(x_j) \Delta x = \sum_{j=1}^N \Phi_{\kappa'}^*(x_j) \Phi_{\kappa}(x_j). \quad (11.155)$$

Taking

$$\Delta x = \frac{L}{N}, \quad x_j = j \Delta x = \frac{jL}{N}, \quad (11.156)$$

the basis orthogonality relation is solved for

$$\Phi_{\kappa}(x_j) = \frac{e^{\sqrt{-1}2\pi\kappa j/N}}{\sqrt{N}} \quad (11.157)$$

(cf. Eqs. 11.149–11.150). Although  $\Phi_{\kappa}(x_j)$  differs from  $\phi_{\kappa}(x_j)$  only in the factor  $\frac{1}{\sqrt{N}}$  versus  $\frac{1}{\sqrt{L}}$ , this difference is important for normalization, and illustrates the general method for calculating the elements of the pseudospectral matrix. The corresponding grid orthogonality relation takes the form (see Exercise 11.19)

$$\sum_{\kappa=-\frac{N}{2}+1}^{\frac{N}{2}} \Phi_{\kappa}(x_i) \Phi_{\kappa}^*(x_j) = \sum_{\kappa=-\frac{N}{2}+1}^{\frac{N}{2}} \frac{e^{\sqrt{-1}2\pi\kappa i/N}}{\sqrt{N}} \frac{e^{-\sqrt{-1}2\pi\kappa j/N}}{\sqrt{N}} = \delta_{ij}. \quad (11.158)$$

### Continuous $k$ -Basis

We now turn to the continuous basis defined by Eq. 11.145. Again, the orthogonal collocation matrix is chosen to make the basis orthogonality relation exact:

$$\begin{aligned} \int_{-\infty}^{\infty} \phi_k^* \phi_{k'}(x) dx &= \int_{-\infty}^{\infty} \frac{e^{i(k-k')x}}{2\pi} dx = \delta(k - k') \\ &= \sum_{j=-\infty}^{\infty} \phi_{k'}^*(x_j) \phi_k(x_j) \Delta x = \sum_{j=-\infty}^{\infty} \Phi_{k'}^*(x_j) \Phi_k(x_j). \end{aligned} \quad (11.159)$$

Taking  $\Delta x = \frac{2\pi}{2K}$ ,  $x_j = j \Delta x = \frac{j\pi}{K}$ , the basis orthogonality relation is satisfied for

$$\Phi_k(x_j) = \frac{e^{ikx_j}}{\sqrt{2K}} \quad (11.160)$$

(see Exercise 11.20). Note that the “matrix” is continuous in the index  $k$  and discrete but infinite in the index  $x_j$ . The corresponding grid orthogonality relation takes the form (see Exercise 11.20)

$$\int_{-K}^K \Phi_k(x_i) \Phi_k^*(x_j) dk = \int_{-K}^K \frac{e^{ik(x_i-x_j)}}{2K} dk = \delta_{ij}. \quad (11.161)$$

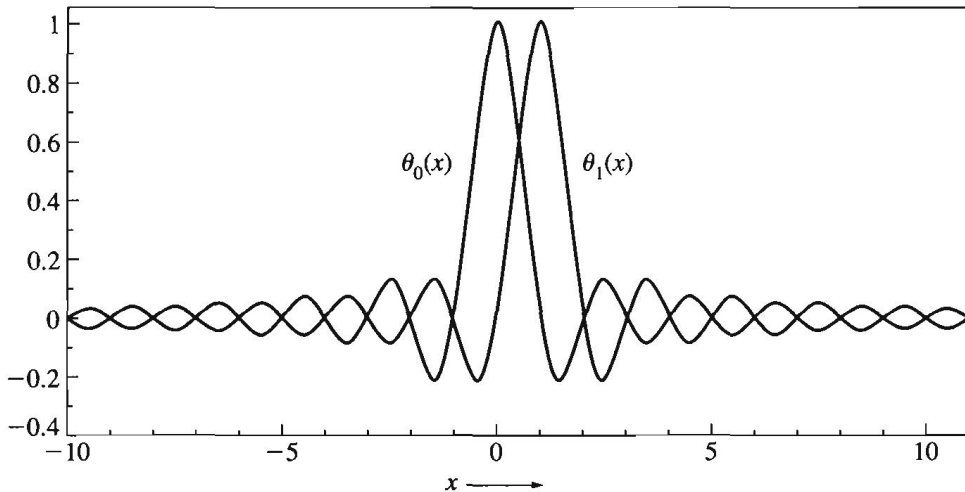


**Figure 11.6** Depiction of the pseudospectral basis functions,  $\theta_j(x) = \text{sinc}[K(x - x_j)]$  in the second variant of the Fourier method (see text). These functions display the characteristic properties of all pseudospectral bases; the basis functions are orthonormal and each basis function vanishes at all grid points except the one where it is centered.

### 11.6.3 Pseudospectral Basis Functions in the Fourier Method

The pseudospectral interpretation of the Fourier method has two variants, corresponding to the two choices of discrete or continuous basis described above. The continuous variant is obtained by substituting Eqs. 11.145 and 11.160 into Eq. 11.43:

$$\begin{aligned} \int_{-K}^K \phi_k(x) \Phi_k^*(x_j) dk &= \theta_j(x) = \int_{-K}^K \frac{e^{ikx}}{\sqrt{2\pi}} \frac{e^{-ikx_j}}{\sqrt{2K}} dk \\ &= \frac{\sin(K(x - x_j))}{\sqrt{\pi K(x - x_j)}} = \sqrt{\frac{K}{\pi}} \text{sinc}[K(x - x_j)] \end{aligned} \quad (11.162)$$

Each sinc function is centered on a different grid point, the space between grid points being  $\Delta x = \frac{\pi}{K}$ . Moreover, the width of each sinc function is approximately  $\frac{\pi}{K}$ .

The behavior of the sinc function is depicted in Figure 11.6. Note that the sinc functions have properties that correspond to those of pseudospectral basis functions in general: they are 1 at their own grid point, vanish at all other grid points, are orthogonal to each other, and form a complete, orthogonal set in a subspace of  $L^2(-\infty, \infty)$  that consists of band-limited functions (functions whose Fourier transforms vanish outside the interval  $[-K, K]$ ). The latter statement will be formalized in the next section, using projection operators. The basis of sinc functions is sometimes called the Hardy basis.

The discrete pseudospectral functions are obtained by substituting Eqs. 11.154 and 11.157 into Eq. 11.158:

$$\sum_{\kappa=-(N/2-1)}^{N/2} \phi_\kappa(x) \Phi_\kappa^*(x_j) = \theta_j(x) = \sum_{\kappa=-(N/2-1)}^{N/2} \frac{e^{i2\pi\kappa x/L}}{\sqrt{L}} \frac{e^{-i2\pi\kappa x_j/L}}{\sqrt{N}}. \quad (11.163)$$

To appreciate the form of the resulting functions, note that the discreteness of the representation in  $k$  implies periodicity in the  $x$ -representation (see Section 6.2); specifically, it implies periodic boundary conditions in  $x$  with period  $L = \frac{\pi}{\Delta k}$ . Thus, the pseudospectral basis functions corresponding to Eq. 11.154 are periodic trains of sinc functions.

### 11.6.4 The Fourier Grid Hamiltonian

The Fourier Grid Hamiltonian (FGH) method (Marston, 1989) refers to the evaluation of the matrix elements of the Hamiltonian using the Fourier pseudospectral scheme. Normally, this matrix is diagonalized to obtain eigenvalues and eigenvectors. The starting point of the FGH is the exact expression for the Hamiltonian operator in the coordinate representation:

$$\langle x | H | x' \rangle = \langle x | T(\hat{p}) + V(\hat{x}) | x' \rangle \quad (11.164)$$

$$\begin{aligned} &= \int_{-\infty}^{\infty} \langle x | k \rangle \frac{\hbar^2 k^2}{2m} \langle k | x' \rangle dk + V(x) \delta(x - x') \\ &= \frac{\hbar^2}{2m} \int_{-\infty}^{\infty} \frac{e^{\sqrt{-1}kx}}{\sqrt{2\pi}} k^2 \frac{e^{-\sqrt{-1}kx'}}{\sqrt{2\pi}} dk + V(x) \delta(x - x'). \end{aligned} \quad (11.165)$$

In the Fourier pseudospectral scheme, the coordinates  $x, x'$  are discretized at  $N$  evenly spaced points,

$$x \rightarrow i \Delta x \quad x' \rightarrow j \Delta x, \quad (11.166)$$

and thus the Hamiltonian matrix in the FGH method is an  $N \times N$  matrix with  $H_{ij}$  corresponding to position  $i \Delta x, j \Delta x$ . (In this section the letter  $i$  is used as an index and we use  $\sqrt{-1}$  for the imaginary number.) The potential energy matrix elements are given by the usual DVR prescription, that the off-diagonal elements vanish and that the diagonal elements are given by the local evaluation of  $V(x)$ :

$$\langle x_i | V(\hat{x}) | x_j \rangle \rightarrow V(x_j) \delta_{ij}. \quad (11.167)$$

The kinetic energy matrix elements take the following form:

$$\langle x_i | T(\hat{p}) | x_j \rangle = \int_{-\infty}^{\infty} \langle x_i | k \rangle \langle k | T(\hat{p}) | k \rangle \langle k | x_j \rangle dk = \frac{\hbar^2}{2m} \int_{-\infty}^{\infty} \frac{e^{\sqrt{-1}ki\Delta x}}{\sqrt{2\pi}} k^2 \frac{e^{-\sqrt{-1}kj\Delta x}}{\sqrt{2\pi}} dk. \quad (11.168)$$

In the FGH method one truncates the range of integration to a region  $[-K, K]$ , where  $K = \pi/\Delta x$ , and discretizes the integral over  $k$ , with the spacing in  $k$  given by  $\Delta k = \frac{2\pi}{N\Delta x}$ , corresponding to the basis implicit in the Fourier pseudospectral scheme. Making the replacement  $k = \kappa \Delta k$  and using the relation

$$\Delta k \Delta x = \frac{2\pi}{N}, \quad (11.169)$$

we obtain

$$\langle x_i | T(\hat{p}) | x_j \rangle \approx \frac{\hbar^2}{2m} \sum_{\kappa=-N/2+1}^{N/2} \frac{e^{\sqrt{-1}2\pi\kappa i/N}}{\sqrt{2K}} (\kappa \Delta k)^2 \frac{e^{-\sqrt{-1}2\pi\kappa j/N}}{\sqrt{2K}} \Delta k \quad (11.170)$$

$$= \frac{\hbar^2}{2m} \left( \frac{2K}{N} \right)^2 \sum_{\kappa=-N/2+1}^{N/2} \frac{e^{\sqrt{-1}2\pi\kappa i/N}}{\sqrt{N}} \kappa^2 \frac{e^{-\sqrt{-1}2\pi\kappa j/N}}{\sqrt{N}} \quad (11.171)$$

(cf. Eq. 11.158 and Exercise 11.19). The summation in Eq. 11.171 can be performed analytically. For  $N$  even, this takes the form

$$\langle x_i | T(\hat{p}) | x_j \rangle = \frac{\hbar^2}{2m} \begin{cases} \frac{K^2}{3} \left(1 + \frac{2}{N^2}\right) & (i = j) \\ \frac{2K^2}{N^2} \frac{(-1)^{j-i}}{\sin^2(\pi \frac{j-i}{N})} & (i \neq j). \end{cases} \quad (11.172)$$

(For  $N$  odd replace the 2 by 1 in the equation for  $i = j$  and add a factor  $\cos(\pi \frac{j-i}{N})$  in the numerator of the equation for  $i \neq j$ .) Note that Eq. 11.171 has the form

$$\langle x_i | T(\hat{p}) | x_j \rangle = \sum_{\kappa=-(N/2-1)}^{N/2} \phi_\kappa(x_j) \frac{\hbar^2 \kappa^2}{2m} \phi_\kappa^*(x_i) = (\mathbf{U}^\dagger \mathbf{T} \mathbf{U})_{ji} \quad (11.173)$$

exactly as in any pseudospectral scheme (cf. Eq. 11.137).

As described above, there is a variation on the original Fourier method in which the underlying basis is taken as  $\frac{e^{\sqrt{-1}kx}}{\sqrt{2\pi}}$ , where  $k$  is a continuous variable,  $k \in [-K, K]$ . This suggests a variation in the FGH method in which the region of integration is truncated *without discretizing  $k$*  (Willner, 2001). Again, the matrix elements can be evaluated analytically, with the resulting  $T$  matrix now taking a somewhat simpler form (Colbert, 1992):

$$\langle x_i | T(\hat{p}) | x_j \rangle \rightarrow \frac{\hbar^2}{2m} \int_{-K}^K \frac{e^{\sqrt{-1}ki\Delta x}}{\sqrt{2K}} k^2 \frac{e^{-\sqrt{-1}kj\Delta x}}{\sqrt{2K}} dk \quad (11.174)$$

$$= \frac{\hbar^2}{2m} \begin{cases} \frac{K^2}{3} & (i = j) \\ \frac{2K^2}{\pi^2} \frac{(-1)^{j-i}}{(j-i)^2} & (i \neq j). \end{cases} \quad (11.175)$$

In the limit  $N \rightarrow \infty$ , Eq. 11.172 is equivalent to Eq. 11.175. Since in the second procedure  $k$  is not discretized, this procedure avoids introducing periodic boundary conditions in  $x$ .

Adding the kinetic and potential energies (Eqs. 11.172 (or 11.175) and 11.167) we obtain

$$\mathbf{H}_{ij}^{\text{FGH}} = \mathbf{T}_{ij}^{\text{FGH}} + \mathbf{V}_{ij}^{\text{FGH}}. \quad (11.176)$$

In principle, the approximation of the FGH matrix is the replacement

$$H \rightarrow H^{\text{FGH}} = P_{\sqcup}(\hat{p}) P_{\sqcap}(\hat{p}) H P_{\sqcap}(\hat{p}) P_{\sqcup}(\hat{p}) \quad (11.177)$$

or

$$H \rightarrow H^{\text{FGH}} = P_{\sqcap}(\hat{p}) H P_{\sqcap}(\hat{p}), \quad (11.178)$$

again depending on the choice of underlying basis. This is in addition to the approximation inherent in the evaluation of the potential energy matrix elements.

### 11.6.5 The Dynamic Fourier Method

The Dynamic Fourier Method (traditionally known as the Fast Fourier Transform, or FFT method), was pioneered by Feit and Fleck (1982) and Kosloff and Kosloff (1983). Although similar in spirit to the Fourier Grid Hamiltonian method, the Dynamic Fourier Method avoids ever constructing the Hamiltonian matrix. Historically, the Dynamic Fourier Method

was the first widely used pseudospectral method in quantum mechanics. It is simple to use, very accurate and very efficient.

In the Dynamic Fourier Method, the operation of  $H\psi$  is calculated as follows:

1. The Hamiltonian operator is partitioned in the usual fashion,  $H = T + V$ . The strategy is to calculate each operator locally. The potential operator is already local in coordinate space, and therefore its operation is simply a multiplication of  $V(x_j)$  by  $\psi(x_j)$ .
2. A local operation of the kinetic energy operator is possible in momentum space where it becomes a multiplication by the kinetic energy discrete spectrum:  $T(k) = \hbar^2 k^2 / 2m$ . Specifically, the kinetic energy operator is calculated by transforming  $\psi$  to momentum space by a backward Discrete Fourier Transform (DFT), multiplying by  $T(k)$  and performing a forward DFT back to coordinate space. (Note that the use of Fourier transforms to calculate derivatives was described in a more general context in Exercise 6.10.)

The explicit matrix–vector representation of  $H\psi = (T + V)\psi$  is as follows:

$$\left\{ \frac{1}{N} \begin{pmatrix} 1 & 1 & 1 & \cdots & 1 \\ 1 & w & w^2 & \cdots & w^{N-1} \\ 1 & w^2 & w^4 & \cdots & w^{2(N-1)} \\ \vdots & \vdots & \vdots & \ddots & \vdots \\ 1 & w^{N-1} & w^{2(N-1)} & \cdots & w^{(N-1)^2} \end{pmatrix} \begin{pmatrix} T_0 & 0 & 0 & \cdots & 0 \\ 0 & T_1 & 0 & \cdots & 0 \\ 0 & 0 & T_2 & \cdots & 0 \\ \vdots & \vdots & \vdots & \ddots & \vdots \\ 0 & 0 & 0 & \cdots & T_{-1} \end{pmatrix} \times \right. \\ \left. \begin{pmatrix} 1 & 1 & 1 & \cdots & 1 \\ 1 & w^{-1} & w^{-2} & \cdots & w^{-(N-1)} \\ 1 & w^{-2} & w^{-4} & \cdots & w^{-2(N-1)} \\ \vdots & \vdots & \vdots & \ddots & \vdots \\ 1 & w^{-(N-1)} & w^{-2(N-1)} & \cdots & w^{-(N-1)^2} \end{pmatrix} + \begin{pmatrix} V(x_0) & 0 & 0 & \cdots & 0 \\ 0 & V(x_1) & 0 & \cdots & 0 \\ 0 & 0 & V(x_2) & \cdots & 0 \\ \vdots & \vdots & \vdots & \ddots & \vdots \\ 0 & 0 & 0 & \cdots & V(x_{N-1}) \end{pmatrix} \right\} \\ \times \begin{pmatrix} \psi(x_0) \\ \psi(x_1) \\ \psi(x_2) \\ \vdots \\ \psi(x_{N-1}) \end{pmatrix}, \quad (11.179)$$

where  $w = e^{2\pi i/N}$ ,  $T_k = \frac{\hbar^2(\kappa\Delta k)^2}{2m}$ , and we have factored out  $\frac{1}{\sqrt{N}}$  from the orthogonal collocation matrices. (Note that  $T_k$  runs over  $[-N/2 + 1, \dots, 0, \dots, N/2]$  but to match the indexing of the FFT matrix the index of  $T$  is shifted to run from  $[0, \dots, N/2, -N/2 + 1, \dots, -1]$ .)

3. Given  $H\psi(x, t_0)$ , the advancement in time may be performed by any of a variety of methods to obtain  $\psi(x, t_1)$ , discussed below. Steps 1–3 are then iterated to obtain  $\psi(t_2)$ , and so on. The use of the DFT, because of its discrete sampling in  $k$ -space, is inextricably linked to periodic boundary conditions in  $x$ , that is, to basis Eq. 11.154, not to basis Eq. 11.145.

In practice, the DFT is implemented by the Fast Fourier Transform (FFT) algorithm, in which the number of multiplications is  $\frac{1}{2}N \ln N$  rather than  $N^2$  for straightforward implementation of the DFT. The use of the FFT gives a significant computational savings

for large vectors. The FFT is based on exploiting the symmetry of the factors  $w^j$ . The basic idea of the FFT involves three steps (see Brigham (1974), Strang (1988); we present the steps here in terms of  $\tilde{\psi} \rightarrow \psi$ , since that is the forward FFT):

1. Split  $\tilde{\psi}$  into  $\tilde{\psi}'$  and  $\tilde{\psi}''$  by separating its even- and odd-numbered components.
2. Transform  $\tilde{\psi}' \rightarrow \psi'$ ,  $\tilde{\psi}'' \rightarrow \psi''$  using the DFT matrix of size  $N/2$ .
3. Construct  $\psi$  from  $\psi'$  and  $\psi''$  using the formulas

$$\psi_j = \psi'_j + w^j \psi''_j, \quad j = 0, \dots, N/2 - 1 \quad (11.180)$$

$$\psi_{j+N/2} = \psi'_j - w^j \psi''_j, \quad j = 0, \dots, N/2 - 1. \quad (11.181)$$

► **Exercise 11.9** Consider the FFT for the case  $N = 4$ . In matrix form, the three steps above can be written as

$$\begin{pmatrix} 1 & 1 & 1 & 1 \\ 1 & i & i^2 & i^3 \\ 1 & i^2 & i^4 & i^6 \\ 1 & i^3 & i^6 & i^9 \end{pmatrix} = \begin{pmatrix} 1 & 0 & 1 & 0 \\ 0 & 1 & 0 & i \\ 1 & 0 & -1 & 0 \\ 0 & 1 & 0 & -i \end{pmatrix} \begin{pmatrix} 1 & 1 & 0 & 0 \\ 1 & -1 & 0 & 0 \\ 0 & 0 & 1 & 1 \\ 0 & 0 & 1 & -1 \end{pmatrix} \begin{pmatrix} 1 & 0 & 0 & 0 \\ 0 & 0 & 1 & 0 \\ 0 & 1 & 0 & 0 \\ 0 & 0 & 0 & 1 \end{pmatrix} \quad (11.182)$$

- Verify that the product of these matrices gives the DFT for  $N = 4$ . Explain why this decomposition corresponds to the three steps described above.
- Verify that each of the  $2 \times 2$  blocks in the middle matrix of the RHS is itself a DFT for  $N = 2$ . Work out the three-step decomposition for each of these  $2 \times 2$  blocks.

The example in Exercise 11.9 illustrates the following general principle: a DFT of size  $N = 2^l$  can be decomposed into a product of three matrices, the middle matrix consisting of two blocks, each of which is a DFT of size  $\frac{N}{2} = 2^{l-1}$ . As a result, the number of multiplications required for a DFT of size  $N$ , instead of being  $N^2$ , is just twice the number required for the DFT of size  $\frac{N}{2}$  (second step) plus  $\frac{N}{2}$  additional multiplications by  $w^j$ ,  $j = 1, \dots, N/2$  (third step). Representing by  $O_N$  the number of operations for the DFT of dimension  $N$ , we have

$$O_N = 2O_{N/2} + \frac{N}{2}. \quad (11.183)$$

Starting with  $O_1 = 0$  and iterating, we find that

$$O_N = \frac{1}{2}Nl = \frac{1}{2}N \ln N. \quad (11.184)$$

► **Exercise 11.10** Verify Eq. 11.184 by induction.

**Solution** Assume that  $O_N = \frac{1}{2}Nl$ . Then  $O_{2N} = \frac{1}{2}(2N)(l+1) = 2(\frac{1}{2}Nl) + N = 2O_N + N$ , consistent with Eq. 11.183. Since  $O_1 = 0$  the assertion is proved.

The Dynamic Fourier Method has two apparent advantages over both the FGH and other methods:

1. By exploiting the FFT algorithm to perform the DFT, the method scales semilinearly with the number of points ( $N \ln N$ ), rather than as  $N^2$  as with matrix multiplication or  $N^3$  as with matrix diagonalization.
2. No matrices are ever constructed or stored. The FFT algorithm works simply by rearranging the elements of the input vector (i.e., the wavefunction).

These advantages of the FFT method should be regarded with some caution, however, since there are ways of obtaining comparable advantages with other methods as well.

### 11.6.6 Phase Space Analysis and the Scaled Fourier Method

In Section 11.1.1 we described a general approach to phase space analysis of spectral and pseudospectral methods. In the case of the Fourier method there is an interesting alternative way to understand the phase space structure (Kosloff, 1993).

In the Fourier method, the maximum wave number,  $K$ , is related to the sampling spacing  $\Delta x$  by  $K = \pi/\Delta x$ . Defining  $k_{\text{range}} = k_{\max} - k_{\min} = 2K$  we have

$$k_{\text{range}} = 2\pi/\Delta x. \quad (11.185)$$

Similarly,

$$x_{\text{range}} = 2\pi/\Delta k. \quad (11.186)$$

Thus, grid *spacing* in coordinate space corresponds to grid *range* in momentum space, and vice versa: grid range in coordinate space corresponds to grid spacing in momentum space. The volume in phase space covered by the Fourier representation is calculated as the product of the range of the grid in coordinate and momentum. Using the relations  $x_{\text{range}} = L$ ,  $\Delta x = L/N$  and  $p_{\text{range}} = \hbar k_{\text{range}}$ , where  $N$  is the number of grid points, we find the phase space volume as

$$\text{volume} = x_{\text{range}} \times p_{\text{range}} = L\hbar/\Delta x = Nh \quad (11.187)$$

(see Figure 11.7a). This simple result has the following appealing interpretation: the volume in phase space is proportional to the number of grid points, where the phase space volume per grid point is Planck's constant. A phase space representation is also useful for analyzing the efficiency of the Fourier method (see Figure 11.7b).

The Fourier method is restricted to evenly spaced grid points, and therefore converges very slowly with respect to the number of grid points for certain problems, such as the Coulomb problem. However, it is possible to perform a nonlinear coordinate transformation that effectively distorts the potential energy function and makes an evenly spaced grid suitable (Fattal, 1996). In one dimension, the original coordinate,  $q$ , is mapped to a new coordinate,  $Q = Q(q, \alpha)$ , where  $\alpha$  is a parameter for the mapping (see Figure 11.8). Wavefunctions are transformed as follows:  $\Psi(Q) = \psi(q(Q))$ . This results in a new scalar product,  $\langle \Psi | \Phi \rangle = \int \Psi^*(Q)\Phi(Q)J dQ = \int \psi^*(q)\phi(q) dq$ , and in  $T = -\frac{\hbar^2}{2m}(J^{-1}(Q)\frac{\partial}{\partial Q})^2$ , where  $J = \frac{\partial q}{\partial Q}$  in one dimension. Clearly, the mapping mixes the coordinates with the ki-

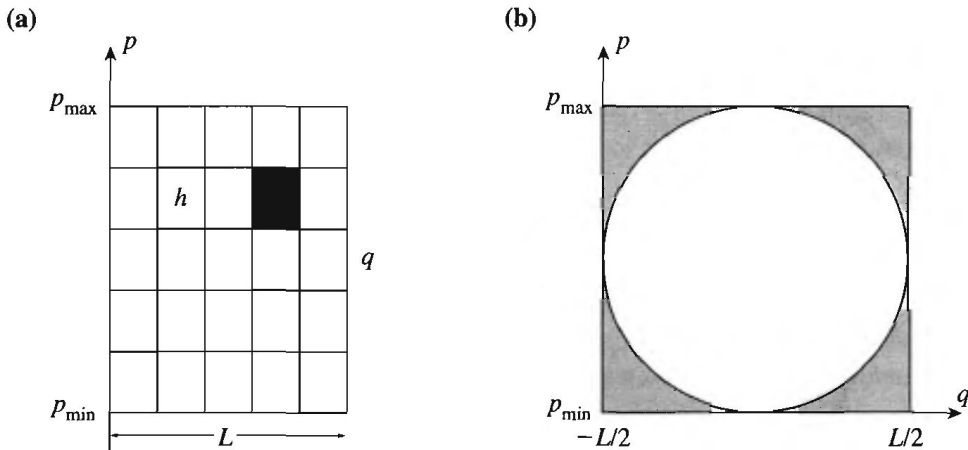


**Figure 11.7** (a) The phase space structure underlying the Fourier method,  $2Lp_{\max} = Nh$ . (b) The Fourier method is based on a square (or rectangular) phase space while for the harmonic oscillator the maximum energy contour is a circle. This implies a maximum efficiency for the Fourier method of  $\pi/4$ . This efficiency limit can be overcome using the mapped Fourier method (see text). Adapted from Kosloff (1993).

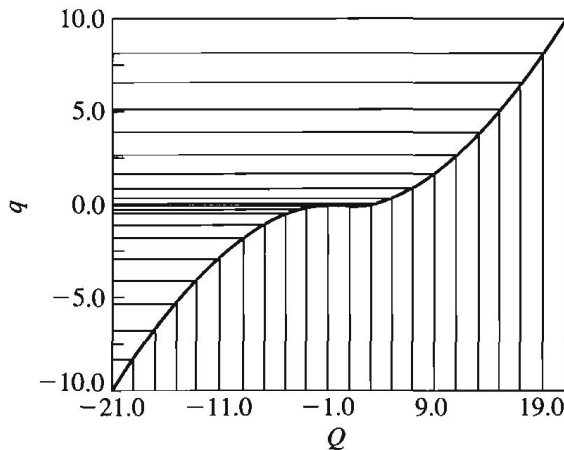


**Figure 11.8** The relation between grids in the Cartesian coordinate system  $q$  and the mapped coordinate  $Q$ , given by the mapping function in the text with  $\beta = 0.1$  and  $A = 9.9$ . Notice the high density of sampling points near the origin of the  $q$ -coordinate, as appropriate for the Coulomb problem. Adapted from Fattal (1996).

netic energy operator, inducing a correlation between the kinetic and the potential energy operators.

For the Coulomb problem the mapping  $q = Q - A \arctan(\beta Q)$  is appropriate. Figure 11.9a shows the phase space included in the energy shells  $n = 1, \dots, 20$  contained within the unscaled grid, while Figure 11.9b shows the portion of the phase space contained within the scaled grid. Here  $p$  is the momentum conjugate to  $q$ , while  $P$  is conjugate to  $Q$ .

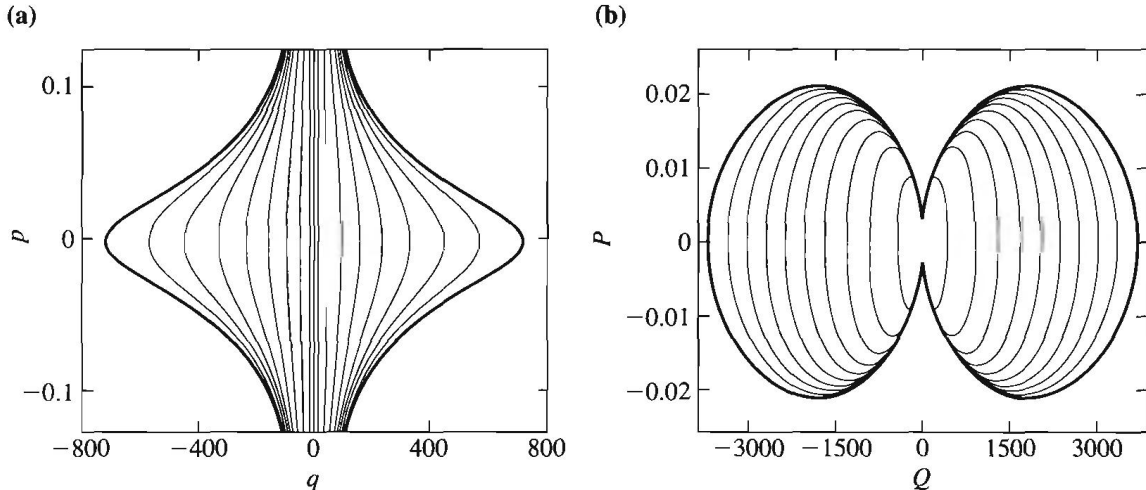


**Figure 11.9** (a) The part of the energy shells  $n = 1, 3, \dots, 20$ , which is represented by the grid rectangle in the unscaled phase space. It is seen that the grid cannot represent the momentum portion of the phase space. (b) The part of the energy shells  $n = 1, 3, \dots, 20$ , which is represented by the grid rectangle in the scaled phase space. The same number of grid points are used as in (a), but now the grid covers all the shells up to  $n = 20$ . Adapted from Fattal (1996).

The mapped Fourier method is an active area of research, with recent ideas exploiting semiclassical concepts of the local de Broglie wavelength to optimize the grid spacing in one and multidimensions (Kokoouline, 1999; Willner, 2002; Goldfarb, 2004).

## 11.7 Time Propagation

So far we have discussed numerical methods for performing the operation  $H\psi$  on a grid of points. We now turn to the question of the numerical implementation of  $e^{-iHt/\hbar}\psi$ . There are three basic strategies for doing this. The first is the straightforward, almost trivial, method of using the approximate eigenvalues and eigenvectors of  $H$  to propagate. The main drawbacks of this approach are that it is limited to time-independent Hamiltonians and it requires the construction and diagonalization of the Hamiltonian matrix, the latter scaling as  $N^3$ . The second approach is to retain the exponent structure of the propagator, but to approximate the propagator as a product of a kinetic and a potential factor (Feit, 1982):

$$e^{-iH\Delta t/\hbar} = e^{-i(\hat{p}^2/2m + V(\hat{x}))\Delta t/\hbar} \quad (11.188)$$

$$\approx e^{-iT\Delta t/\hbar} e^{-i(V\Delta t/\hbar)}, \quad (11.189)$$

where  $T = \hat{p}^2/2m$ . This approach is called the “Split Operator” method, and explicitly preserves unitarity. The third major strategy is to consider  $e^{-iHt/\hbar}$  as a function of the Hamiltonian, that is,  $f(H)$ , and look for a suitable polynomial approximation to this function (Leforestier, 1991; Kosloff, 1994):

$$e^{-iHt/\hbar} \approx \sum_{n=0}^N c_n P_n(H). \quad (11.190)$$

Because we know how to calculate  $H\psi$ , for example by pseudospectral methods, we can calculate  $H(H\psi)$  and ultimately  $H^n\psi$  for any  $n$  by iteration; therefore,  $P_n(H)\psi$  can be calculated for any polynomial of  $H$ . There are many variations on the third approach (some of which do not even look superficially to be in this form), which differ in the choice of the polynomial used. Below, we describe in more detail all of these propagation strategies.

### 11.7.1 The Split Operator Method

The Split Operator method is one of the simplest and most popular methods for time propagation of wavepackets (Feit, 1982). The method begins by representing the propagator over the global time interval  $[0, t]$  as a product of propagators over short time intervals,  $\Delta t$ , where  $N\Delta t = t$ . Thus,

$$U(t, 0) = e^{-iHt/\hbar} = \underbrace{e^{-iH\Delta t/\hbar} e^{-iH\Delta t/\hbar} \dots e^{-iH\Delta t/\hbar}}_{N \text{ times}}. \quad (11.191)$$

The strategy is then to approximate each short time propagator as a product of a kinetic factor and a potential factor:

$$\begin{aligned} e^{-iH\Delta t/\hbar} &= e^{-i(\hat{p}^2/2m + V(\hat{x}))\Delta t/\hbar} \\ &\approx e^{-i(T\Delta t/\hbar)} e^{-i(V\Delta t/\hbar)} + O(\Delta t^2), \end{aligned} \quad (11.192)$$

where  $T = \hat{p}^2/2m$ . Note that this product representation would be exact if  $T$  and  $V$  commuted; we expect the error, therefore, to be proportional to the commutator  $[T, V]$ .

► **Exercise 11.11** Find the leading order corrections and show that they are indeed  $O(\Delta t^2)$  and proportional to  $[T, V]$ .

**Solution** Expand  $e^{-i(T+V)\Delta t/\hbar}$ :

$$\begin{aligned} e^{-i(T+V)\Delta t/\hbar} &= \mathbf{1} - i(T+V)\frac{\Delta t}{\hbar} + \frac{(-i)^2(T+V)^2 \Delta t^2}{2\hbar^2} + \dots \\ &= \mathbf{1} - i(T+V)\frac{\Delta t}{\hbar} - \frac{(T^2 + V^2 + TV + VT) \Delta t^2}{2\hbar^2} + \dots \end{aligned} \quad (11.193)$$

Now expand  $e^{-i(T\Delta t/\hbar)} e^{-i(V\Delta t/\hbar)}$ :

$$\begin{aligned} e^{-i(T\Delta t/\hbar)} e^{-i(V\Delta t/\hbar)} &= \left( \mathbf{1} - iT\frac{\Delta t}{\hbar} + \frac{(-iT\Delta t)^2}{2\hbar^2} + \dots \right) \left( \mathbf{1} - iV\frac{\Delta t}{\hbar} + \frac{(-iV\Delta t)^2}{2\hbar^2} + \dots \right) \\ &= \mathbf{1} - iT\frac{\Delta t}{\hbar} - iV\frac{\Delta t}{\hbar} - \frac{T^2\Delta t^2}{2\hbar^2} - \frac{V^2\Delta t^2}{2\hbar^2} - TV\frac{\Delta t^2}{\hbar^2} + \dots \end{aligned} \quad (11.194)$$

Comparing the approximation, Eq. 11.194, with the exact expression, Eq. 11.193, we see that the error is

$$\text{Error} = \frac{TV - VT}{2} \frac{\Delta t^2}{\hbar^2} + \dots = \frac{[T, V]}{2} \frac{\Delta t^2}{\hbar^2} + \dots \quad (11.195)$$

It is easily verified that choosing the opposite order of the products,

$$e^{-iH\Delta t/\hbar} \approx e^{-i(V\Delta t/\hbar)} e^{-i(T\Delta t/\hbar)} \quad (11.196)$$

gives the same order of error. However, the leading order error can be eliminated by forming a symmetrized product of the kinetic and potential factors:

$$\begin{aligned} e^{-iH\Delta t/\hbar} &\approx \{e^{-i(V\Delta t/2\hbar)} e^{-i(T\Delta t/2\hbar)}\} \{e^{-i(T\Delta t/2\hbar)} e^{-i(V\Delta t/2\hbar)}\} + O(\Delta t^3) \\ &= e^{-i(V\Delta t/2\hbar)} e^{-i(T\Delta t/\hbar)} e^{-i(V\Delta t/2\hbar)} + O(\Delta t^3) \end{aligned} \quad (11.197)$$

► **Exercise 11.12** Find the leading order corrections to the symmetrized product and show that they are indeed  $O(\Delta t^3)$ .

**Solution** Expand  $e^{-i(T+V)\Delta t/\hbar}$ :

$$\begin{aligned} e^{-i(T+V)\Delta t/\hbar} &= 1 - i(T+V) \frac{\Delta t}{\hbar} + \frac{(-i)^2(T+V)^2 \Delta t^2}{2\hbar^2} + \frac{(-i)^3(T+V)^3 \Delta t^3}{3!\hbar^3} + \dots \\ &= 1 - i(T+V) \frac{\Delta t}{\hbar} - \frac{(T^2 + V^2 + TV + VT) \Delta t^2}{2\hbar^2} \\ &\quad + i \frac{(T^3 + TVT + T^2V + TV^2 + VT^2 + V^2T + VTV + V^3)}{3!\hbar^3} + \dots \end{aligned} \quad (11.198)$$

Now expand  $e^{-iV\Delta t/2\hbar} e^{-iT\Delta t/\hbar} e^{-iV\Delta t/2\hbar}$ :

$$\begin{aligned} &e^{-iV\Delta t/2\hbar} e^{-iT\Delta t/\hbar} e^{-iV\Delta t/2\hbar} \\ &= \left[ 1 - iV \frac{\Delta t}{2\hbar} + \frac{(-iV\Delta t)^2}{8\hbar^2} + \dots \right] \left[ 1 - iT \frac{\Delta t}{\hbar} + \frac{(-iT\Delta t)^2}{2\hbar^2} + \dots \right] \\ &\quad \times \left[ 1 - iV \frac{\Delta t}{2\hbar} + \frac{(-iV\Delta t)^2}{8\hbar^2} + \dots \right] \\ &= 1 - i(T+V) \frac{\Delta t}{\hbar} - \frac{(T^2 + V^2 + TV + VT) \Delta t^2}{2\hbar^2} \\ &\quad + i \left( \frac{V^3}{6} + \frac{T^3}{6} + \frac{VTV}{4} + \frac{V^2T}{8} + \frac{VT^2}{4} + \frac{T^2V}{4} + \frac{TV^2}{8} \right) \frac{\Delta t^3}{\hbar^3} + \dots \end{aligned} \quad (11.199)$$

Comparing the approximation, Eq. 11.199, with the exact expression, Eq. 11.198, we see that the error of  $O(\Delta t^2)$  vanishes and the leading error term is

$$\begin{aligned} \text{Error} &= i \frac{\Delta t^3}{\hbar^3} \left( \frac{T[V, T]}{12} + \frac{[T, V]T}{12} + \frac{[T, V], V}{24} + \frac{V[V, T]}{24} \right) \\ &= i \frac{\Delta t^3}{\hbar^3} \left( \frac{[T, [V, T]]}{12} + \frac{[V, [V, T]]}{24} \right). \end{aligned} \quad (11.200)$$

When multiple time steps are concatenated, the half-time steps with evolution under  $V$  coalesce, and one obtains

$$\begin{aligned}
 e^{-iHt/\hbar} &= \\
 &\underbrace{\{e^{-i(V\Delta t/2\hbar)}e^{-i(T\Delta t/\hbar)}e^{-i(V\Delta t/2\hbar)}\}\{e^{-i(V\Delta t/2\hbar)}e^{-i(T\Delta t/\hbar)}e^{-i(V\Delta t/2\hbar)}\}\dots}_{N \text{ times}} \\
 &= \underbrace{e^{-i(V\Delta t/2\hbar)}e^{-i(T\Delta t/\hbar)}e^{-i(V\Delta t/\hbar)}e^{-i(T\Delta t/\hbar)}e^{-i(V\Delta t/\hbar)}\dots}_{N-1 \text{ times}} \\
 &\quad \underbrace{e^{-i(T\Delta t/\hbar)}e^{-i(V\Delta t/\hbar)}e^{-i(T\Delta t/\hbar)}e^{-i(V\Delta t/2\hbar)}}_{\text{.}}
 \end{aligned} \tag{11.201}$$

The operation  $e^{-iV(\hat{x})\Delta t/\hbar}\psi$  is calculated by multiplication,  $e^{-iV(x)\Delta t/\hbar}\psi(x)$ ; and  $e^{-iT(\hat{p})\Delta t/\hbar}\psi = e^{-i\hat{p}^2\Delta t/2m\hbar}\psi$  is calculated by  $Z e^{-ip^2\Delta t/2m\hbar} Z^\dagger \psi(x)$ , where  $Z^\dagger$  is the transformation between the coordinate and momentum representations. In most applications the Split Operator method is implemented in the Fourier basis. In the Fourier basis  $Z^\dagger$  is just a Discrete Fourier Transform (matrix elements of the form  $Z_{ij}^\dagger = \frac{1}{\sqrt{N}} e^{i p_i x_j / \hbar}$ ), which may be calculated very efficiently using an FFT. However, it is worth noting that the Split Operator method is not limited to the Fourier basis; in fact it can be used with other spectral bases provided that the Discrete Fourier Transform is replaced by the corresponding pseudospectral  $\leftrightarrow$  spectral transformation matrix. The Split Operator method is manifestly unitary, and is recommended whenever the Hamiltonian can be written as a sum of operators that depend on coordinates and operators that depend on momenta. However, the method cannot handle operators that mix coordinates and momenta, such as an operator of the form  $e^{i\hat{p}\hat{x}}$ .

The Split Operator method may still be used, but requires slightly more work if the dynamics is evolving on multiple electronic states. At every time step, in addition to transforming between the coordinate and momentum representations, the coordinate space wavefunction has to be transformed into a representation in which the potential is diagonal. For two electronic states this transformation can be performed analytically. Since this is a common case we present the algebra explicitly (Schwendner, 1997). Consider the two-electronic-state evolution operator:

$$\begin{aligned}
 \exp\left[-\frac{i}{\hbar}\begin{pmatrix} T + V_1 & V_{12} \\ V_{21} & T + V_2 \end{pmatrix}\Delta t\right] &= \\
 \exp\left[-\frac{i}{\hbar}\begin{pmatrix} T & 0 \\ 0 & T \end{pmatrix}\frac{\Delta t}{2}\right] \exp\left[-\frac{i}{\hbar}\begin{pmatrix} V_1 & V_{12} \\ V_{21} & V_2 \end{pmatrix}\Delta t\right] \exp\left[-\frac{i}{\hbar}\begin{pmatrix} T & 0 \\ 0 & T \end{pmatrix}\frac{\Delta t}{2}\right] \\
 &+ O(\Delta t^3).
 \end{aligned} \tag{11.202}$$

The complication arises since the potential energy,  $V$ , is now a matrix, and is no longer diagonal. This difficulty can be overcome by transforming the  $2 \times 2$  potential matrix into a representation in which it is diagonal, and then transforming back after the multiplication operation on the wavefunction is performed. For a  $2 \times 2$  Hermitian matrix this transformation can be done analytically (see Exercise 8.74). Note that since the  $V$  matrix is coordinate

dependent, so is the transformation matrix,  $U$ , that diagonalizes it. Denoting this matrix by  $U$ , since  $U$  is unitary we can write

$$\begin{aligned} & \exp \left[ -\frac{i}{\hbar} \begin{pmatrix} V_1 & V_{12} \\ V_{21} & V_2 \end{pmatrix} \Delta t \right] \\ &= U \exp \left[ -\frac{i}{\hbar} U^\dagger \begin{pmatrix} V_1 & V_{12} \\ V_{21} & V_2 \end{pmatrix} U \Delta t \right] U^\dagger = U \begin{pmatrix} e^{-\frac{i}{\hbar} \lambda_1 \Delta t} & 0 \\ 0 & e^{-\frac{i}{\hbar} \lambda_2 \Delta t} \end{pmatrix} U^\dagger \end{aligned} \quad (11.203)$$

$$= \exp \left[ -\frac{i}{\hbar} (V_1 + V_2) \frac{\Delta t}{2} \right] \left[ \cos \left( \sqrt{D} \frac{\Delta t}{2\hbar} \right) \begin{pmatrix} 1 & 0 \\ 0 & 1 \end{pmatrix} + i \frac{\sin(\sqrt{D} \frac{\Delta t}{2\hbar})}{\sqrt{D}} \begin{pmatrix} V_2 - V_1 & -2V_{12} \\ -2V_{21} & V_1 - V_2 \end{pmatrix} \right], \quad (11.204)$$

where we have used the result of Exercise 8.74.

► **Exercise 11.13** Verify Eq. 11.204.

Equation 11.204 is in a convenient form for numerical work, requiring only straightforward matrix multiplication. Combined with Eq. 11.202, it gives a full prescription for the Split Operator propagator for the two-surface case. For three or more potentials, however, there is no such simple analytical transformation, and a numerical matrix diagonalization must be done for every coordinate. For time-independent potentials, this numerical diagonalization does not need to be repeated at every time step, but can be performed once at the beginning of the propagation and the transformation matrices stored. However, for time-dependent potentials—for example, evolution in the presence of pulsed laser fields—the diagonalization must be performed at every time step.

### 11.7.2 Symplectic Integrators

Symplectic integrators are integrators that respect the symplectic symmetry properties of a dynamical system; they preserve the canonical relationship between  $p$  and  $q$ . Such integrators have been widely used in classical mechanics, and less so in quantum mechanics. Recently, some encouraging preliminary applications of these integrators to quantum mechanics have been demonstrated (Gray, 1996).

The starting point is that the Time-Dependent Schrödinger Equation can be written in discrete form as

$$i \frac{d}{dt} c(t) = H \cdot c(t). \quad (11.205)$$

Take  $H$  to be a real symmetric, time-independent matrix. Define

$$q(t) = \sqrt{2} \operatorname{Re}(c(t)), \quad p(t) = \sqrt{2} \operatorname{Im}(c(t)), \quad (11.206)$$

and the Hamiltonian function

$$h(q, p) = \frac{1}{2} \sum_{ij} H_{ij} (p_i p_j + q_i q_j). \quad (11.207)$$

Then Eq. 11.205 is equivalent to the equations

$$\frac{d}{dt}q(t) = \frac{\partial}{\partial p}h(q, p) = H \cdot p, \quad (11.208)$$

$$\frac{d}{dt}p(t) = -\frac{\partial}{\partial q}h(q, p) = -H \cdot q, \quad (11.209)$$

which are just Hamilton's equations for a large set of quadratically coupled harmonic oscillators.  $h(q, p)$  has the physical interpretation of the mean wavepacket energy. A discrete procedure for integrating these equations is

$$p_j = p_{j-1} - b_j \tau H \cdot q_{j-1}, \quad (11.210)$$

$$q_j = q_{j-1} + a_j \tau H \cdot p_j, \quad j = 1, 2, \dots, m. \quad (11.211)$$

Equation 11.211 involves numerical work equivalent to  $2m$  evaluations of  $H$  on a real vector, but the evolution matrix contains terms up to  $(H\tau)^{2m}$ . In essence, what makes Eq. 11.211 symplectic is the use of  $p_j$  and not  $p_{j-1}$  in the determination of  $q_j$  at each iteration.

### 11.7.3 Polynomial Methods

Polynomial methods represent the propagator as  $e^{-iHt/\hbar}\psi = \sum_n a_n P_n(H)\psi$ , where  $P_n(H)$  is some polynomial of the Hamiltonian operator. Once a polynomial sequence is chosen, the  $a_n$  are uniquely determined. Polynomial methods can be divided into two categories: those that choose the polynomial in advance, and those that do not (Leforestier, 1991; Kosloff, 1994). An example of a method that chooses the polynomial in advance is the Chebyshev method (Tal-Ezer, 1984). An example of the second type of polynomial expansion is the Short Iterative Lanczos propagator (Park, 1986). We now discuss both of these methods in some detail.

#### Chebyshev Propagation

For functions of scalar arguments,  $f(x)$ ,  $x$  in the interval  $[-1, 1]$ ,  $f(x) = \sum a_n P_n(x)$ , the representation in terms of  $N$  Chebyshev polynomials minimizes the maximum error in the representation of the function over the interval. This minimization of the maximum error allows the use of Chebyshev polynomials to reach the level of machine accuracy in numerical computations.

Since we are interested in expanding the propagator in terms of Chebyshev polynomials, we are interested in the representation of exponential functions in terms of Chebyshev polynomials. For exponential functions this expansion takes the specific form

$$e^{-i\alpha x} = \sum a_n(\alpha) \Phi_n(-ix), \quad (11.212)$$

where

$$a_n(\alpha) = \int_{-i}^i \frac{e^{i\alpha x} \Phi_n(x) dx}{(1-x^2)^{1/2}} = 2J_n(\alpha) \quad (11.213)$$

with

$$a_0(\alpha) = J_0(\alpha), \quad (11.214)$$

where the  $J_n(\alpha)$  are Bessel functions. The Chebyshev recurrence relation is

$$\Phi_{n+1} = -2ix\Phi_n + \Phi_{n-1}. \quad (11.215)$$

In implementing this expansion for the propagator, the argument  $-iHt/\hbar$  must first be mapped onto the domain  $[-i, i]$ :

$$H_{\text{norm}} = 2 \frac{H - I(\Delta E_{\text{grid}}/2 + E_{\min})}{\Delta E_{\text{grid}}}, \quad (11.216)$$

where  $\Delta E_{\text{grid}} = E_{\max} - E_{\min}$  is the range of energy supported by the grid. Here,  $E_{\max} = V_{\max} + T_{\max}$  and  $E_{\min} = V_{\min}$  are the maximum and minimum energy supported by the grid, and  $T_{\max} = \hbar^2 k_{\text{range}}^2 / 2m$  is the maximum kinetic energy supported by the grid, with  $k_{\text{range}} = \pi / \Delta x$ . With this mapping, the wavefunction is given by

$$\psi(t) \approx e^{-i(E_{\min}t/\hbar + \alpha)} \sum_n a_n(\alpha) \Phi_n(-iH_{\text{norm}}) \psi(0), \quad (11.217)$$

where the  $\Phi_n$  are the complex Chebyshev polynomials and  $\alpha = \frac{\Delta E_{\text{grid}} t}{2\hbar}$ . The polynomials are generated by the recurrence relation,

$$\phi_{n+1} = -2iH_{\text{norm}}\phi_n + \phi_{n-1}, \quad (11.218)$$

where

$$\phi_n = \Phi_n(-iH_{\text{norm}})\phi(0); \quad (11.219)$$

the recurrence is started with

$$\phi_0 = \psi(0) \quad (11.220)$$

and

$$\phi_1 = -iH_{\text{norm}}\psi(0). \quad (11.221)$$

The Chebyshev propagator effectively does the propagation in a single time step, and intermediate time results are not automatically obtained. However, since all the time dependence and none of the spatial dependence is in the Bessel function coefficients, once the calculation of the Chebyshev polynomials is done, information at any intermediate time can be obtained cheaply. Similarly, time-correlation functions can be obtained by calculating the overlaps of the Chebyshev polynomials with the wavefunction of interest, and then weighting these time-independent overlaps by Bessel functions of time-dependent arguments.

### Short Iterative Lanczos Propagator

As an example of the second type of polynomial expansion, one for which the polynomial is not determined in advance, we consider the Short Iterative Lanczos propagator. We first introduce the concept of a Krylov space. This is a subspace of the full Hilbert space, obtained by acting with a linear operator on an initial state  $N$  times. For example, if the linear operator is the Hamiltonian, the Krylov space is spanned by the vectors  $u_j = H^j \psi(0)$ . The Lanczos method constructs a matrix representation of the Hamiltonian in a basis spanned by the Krylov space; the Hamiltonian matrix is then diagonalized and the diagonal representation

is used to propagate the initial state within the Krylov space. Since the operator  $H$  is used to build the Krylov space, the Krylov space is in fact tailored to include that portion of the Hilbert space that the wavefunction explores in the near future.

The functions that define the Krylov space,  $u_j = H^j \psi(0)$ , are generally not orthogonal. However, in practice, it is usually more convenient to work with orthogonal functions. In the Lanczos method, as each new Krylov vector is constructed it is also orthogonalized to the previous Krylov vectors. Specifically, the first basis function,  $q_0$ , is just the initial state itself:

$$q_0 = \psi(0). \quad (11.222)$$

The second basis function,  $q_1$ , is determined by operating with  $H$  on  $q_0$ , and subtracting off the component of  $q_0$  in the result:

$$Hq_0 = \alpha_0 q_0 + \beta_0 q_1, \quad (11.223)$$

where  $\alpha_0 = \langle q_0 | H | q_0 \rangle$  and  $\beta_0 = \langle q_1 | H | q_0 \rangle$ . The third member of the basis,  $q_2$ , is determined by operating with  $H$  on  $q_1$ , and subtracting off the component of both  $q_1$  and  $q_0$  in the result:

$$Hq_1 = \beta_0 q_0 + \alpha_1 q_1 + \beta_1 q_2, \quad (11.224)$$

where  $\alpha_1 = \langle q_1 | H | q_1 \rangle$  and  $\beta_1 = \langle q_2 | H | q_1 \rangle$ . The general expression takes the form

$$Hq_j = \beta_{j-1} q_{j-1} + \alpha_j q_j + \beta_j q_{j+1}, \quad (11.225)$$

where the coefficients are given by

$$\alpha_j = \langle q_j | H q_j \rangle \quad (11.226)$$

and

$$\beta_{j-1} = \langle q_j | H q_{j-1} \rangle. \quad (11.227)$$

The striking feature of the general expression is that it never has more than three terms; for example,  $Hq_2$  has no  $q_0$  term. This is a direct result of Hermiticity: since  $\langle q_2 | H | q_0 \rangle = 0$  (which can be seen by taking the inner product of Eq. 11.223 with  $q_2$ ), it follows that  $\langle q_0 | H | q_2 \rangle$  must also be zero. We now note that the various coefficients in Eqs. 11.223, 11.224, and 11.225 are matrix elements of the Hamiltonian operator in the Lanczos basis. This matrix is evidently tridiagonal, and takes the following form:

$$H_N = \begin{pmatrix} \alpha_0 & \beta_0 & 0 & \cdots & \cdots & \cdots & 0 \\ \beta_0 & \alpha_1 & \beta_1 & 0 & \cdots & \cdots & 0 \\ 0 & \beta_1 & \alpha_2 & \beta_2 & 0 & \cdots & 0 \\ \vdots & \vdots & \ddots & \ddots & \vdots & \vdots & 0 \\ 0 & \cdots & \cdots & \cdots & \beta_{N-3} & \alpha_{N-2} & \beta_{N-2} \\ 0 & \cdots & \cdots & \cdots & \cdots & \beta_{N-2} & \alpha_{N-1} \end{pmatrix}, \quad (11.228)$$

where we have assumed the Hermiticity of the matrix to equate the lower and upper half of the  $H$  matrix.

► **Exercise 11.14** According to Eq. 11.225,  $Hq_2 = \beta_1 q_1 + \alpha_2 q_2 + \beta_2 q_3$ . Show explicitly that the coefficient of  $q_1$  is indeed the same as  $\beta_1$  defined by Eq. 11.224.

**Solution** Define the quantity  $\gamma_1 \equiv \langle q_1 | H q_2 \rangle$ . The task then is to show that  $\gamma_1 = \beta_1$  as defined by Eq. 11.224. We have

$$\begin{aligned}\gamma_1 &= \langle q_1 | H q_2 \rangle \\ &= \left\langle q_1 | H \right| \frac{H q_1 - \alpha_1 q_1}{\beta_1} \\ &= \frac{\langle q_1 | H^2 | q_1 \rangle - \alpha_1 \langle q_1 | H | q_1 \rangle}{\beta_1},\end{aligned}\quad (11.229)$$

where we have used the definition of  $q_2$  from Eq. 11.224. Since  $q_2$  is assumed to be normalized, we have from Eq. 11.224

$$\begin{aligned}\beta_1^2 &= \langle H q_1 - \alpha_1 q_1 | H q_1 - \alpha_1 q_1 \rangle \\ &= \langle q_1 | H^2 | q_1 \rangle - 2\alpha_1 \langle q_1 | H | q_1 \rangle + \alpha_1^2 \\ &= \langle q_1 | H^2 | q_1 \rangle - \alpha_1 \langle q_1 | H | q_1 \rangle,\end{aligned}\quad (11.230)$$

where we have used the relation  $\alpha_1 = \langle q_1 | H | q_1 \rangle$ . Dividing both sides of Eq. 11.230 by  $\beta_1$  and comparing with Eq. 11.229 completes the proof.

► **Exercise 11.15** Use a similar approach to show explicitly that  $\langle q_1 | H q_3 \rangle = 0$ .

Diagonalization of the matrix representation of the Hamiltonian gives

$$Z^\dagger H_N Z = D_N, \quad (11.231)$$

where  $D_N$  is a diagonal matrix of eigenvalues of  $H_N$ . Using the transformation matrix  $Z$ , one obtains the following expression for the propagator:

$$U(\Delta t) = e^{-i H_N \Delta t / \hbar} = Z e^{-i Z^\dagger D_N Z \Delta t / \hbar} Z^\dagger = Z e^{-i D_N \Delta t / \hbar} Z^\dagger. \quad (11.232)$$

The propagated wavefunction is then given by

$$\psi(\Delta t) = Z e^{-i D_N \Delta t / \hbar} Z^\dagger \psi(0). \quad (11.233)$$

Note that in the Lanczos basis, the initial state  $\psi(0)$  is just the column vector  $(1, 0, \dots, 0)^T$ . Hence, if we view  $Z e^{-i D_N \Delta t / \hbar} Z^\dagger$  as an  $N \times N$  matrix, only the first column of this matrix affects the calculation of  $\psi(\Delta t)$ .

We have commented above that the Krylov space spanned by  $u_j = H^j \psi(0)$  spans that subspace of the Hilbert space where  $\psi(0)$  will evolve in short times. The reasoning is that this is the same subspace spanned by the Taylor series expansion of the propagator, which is valid at short times. The size of the Krylov space determines the time for which the evolving wavepacket will be confined within the Krylov space; the larger the Krylov space generated, the longer it should be able to describe the packet dynamics. Indeed, one can show that for a finite Hilbert space—an  $N$ -level system—a Krylov space of size  $N$  generates the exact dynamics, within numerical error. In practice, there is a trade-off between generating a large

Krylov space and using it for long time step propagation, and generating a small Krylov space but using it for short time steps and updating it frequently, generating a new Krylov space with the current initial state. The latter is called the Short Iterative Lanczos method. There is some empirical evidence that the optimal numerical efficiency is obtained with a Krylov space whose dimension is between six and twenty, depending on the system. The Short Iterative Lanczos method can be used with a variable time step. A convenient way to estimate the time step is to calculate the quantity  $\|\frac{\partial}{\partial t} - \frac{H}{i\hbar}\psi(0)\|$ , where  $\frac{\partial\psi}{\partial t}$  is obtained as the finite difference between  $\psi(\Delta t)$  calculated by the Lanczos method and  $\psi(t)$ . The difference between these two quantities is an estimate of the numerical error; by calculating this quantity and maintaining it below a desired error tolerance, one can propagate with an adaptive step size.

#### 11.7.4 Spectral Analysis of Time-Correlation Functions

The goal of wavepacket propagation is often to calculate some form of energy-resolved transition probability. This transition probability may be, for example, an absorption spectrum,  $\sigma(E)$ , or a scattering matrix element,  $S_{\beta\alpha}(E)$ . These transition probabilities, as well as many others, can be formulated as Fourier transforms of wavepacket time-correlation functions, that is,  $\sigma(E) = \int_{-\infty}^{\infty} C(t) e^{iEt/\hbar} dt$ . Thus, one is often in a situation of having a time signal of some form and wanting to know its Fourier transform.

Conventional wisdom is that the maximum resolution of the frequency spectrum is determined by the length of the time signal according to the time-energy uncertainty principle,  $\Delta E \approx \hbar/T$ . This is true if the frequency points are evenly spaced. However, if the actual spectrum has detailed structure in some regions and is flat in other regions a set of evenly spaced frequencies will not be optimal and it is possible to do much better than the uncertainty principle limit. We describe in this section a remarkable method for obtaining high-resolution spectra from short time signals. The method does not actually violate the uncertainty principle, but simply circumvents it, essentially by exploiting prior information on the functional form of the time signal. The method can be applied not only to calculations but also to experimental data, providing high-resolution spectral information from a short time signal.

The usual way to construct a frequency spectrum from a time signal is via a Discrete Fourier Transform (DFT):

$$\sigma(\omega_m) = \sum_{n=1}^N C(t_n) e^{i\omega_m t_n}, \quad (11.234)$$

where the  $t_n$  are the times at which the signal is known. In the DFT, the frequencies  $\omega_m$  are specified *a priori*; since we assume no *a priori* knowledge of the spectrum, the  $\omega_m$  are usually taken to be evenly spaced. The DFT amplitudes can then be viewed as the optimal solution (in a least squares sense) to the following fitting problem: find the set of  $\sigma(\omega_m)$ ,  $m = 1, \dots, N$ , such that

$$C(t_n) = \frac{1}{N} \sum_{m=1}^N \sigma(\omega_m) e^{-i\omega_m t_n}. \quad (11.235)$$

The equivalence of Eqs. 11.234 and 11.235 follows from the properties of the inverse DFT (see Eq. 6.54). A consequence of the use of evenly spaced points is indeed that the highest frequency resolution possible in the DFT is given by the uncertainty principle,  $\Delta E \approx \hbar/T$ , where  $T$  is the length of the time signal.

Consider now allowing both the frequencies and the amplitudes to be optimized. Writing the signal as

$$C(t_n) = \sum_{k=1}^K d_k e^{-i\omega_k t_n}, \quad n = 1, 2, \dots, N, \quad (11.236)$$

if the number  $N$  of sampling points in time is larger than the number  $2K$  of unknowns contributing to the signal, which consists of  $K$  frequencies  $\omega_k$  with their amplitudes  $d_k$ , one should be able in principle to extract all the unknowns. This problem, sometimes called “harmonic inversion,” is a fundamental problem in physics, electrical engineering and many other diverse fields. Unfortunately, as opposed to the DFT, the harmonic inversion problem with variable frequencies is a nonlinear fitting problem.

In this section we describe a new and efficient approach to this fitting problem that has recently emerged from the literature on wavepacket correlation functions. The approach, invented by Wall and Neuhauser (WN) in terms of continuous time signals (Wall, 1995) and later reformulated by Mandelshtam and Taylor (MT) in terms of discrete time signals (Mandelshtam, 1997), involves two crucial ideas. The first is to associate the signal  $C(t)$  with an autocorrelation function of a dynamical system:

$$C(t) = \langle \Phi_0 | e^{-it\hat{\Omega}} | \Phi_0 \rangle. \quad (11.237)$$

This establishes an equivalence between the problem of extracting spectral information from the signal with the one of diagonalizing the evolution operator  $e^{-it\hat{\Omega}}$  of the underlying dynamical system. Because the operator  $e^{-it\hat{\Omega}}$  has restrictions on the form of its eigenvalues and eigenfunctions, Eq. 11.237 is equivalent to assuming something about the functional form of the time signal.

The second crucial idea is that neither the identity of the operator  $e^{-it\hat{\Omega}}$  nor the basis functions need be known explicitly: the matrix elements of  $e^{-it\hat{\Omega}}$  can be expressed in terms of  $C(t)$  alone. Essentially, the one-dimensional sequence  $C(t)$  is converted to a two-dimensional array; the latter can be diagonalized, so that the original nonlinear fitting problem has been transformed into a standard problem in linear algebra. Note that from the point of view of information content the matrix contains no more information than the original sequence  $C(t)$ , but it doesn't need to: the final goal is a set of  $2K$  parameters (the  $K$  eigenvalues and  $K$  overlaps of the eigenvectors), which is a one-dimensional sequence.

To develop the first idea, we express the evolution operator,  $e^{-it\hat{\Omega}}$ , in terms of its eigenvalues and eigenvectors:

$$e^{-it\hat{\Omega}} = \sum_{k=1}^K e^{i\omega_k t} |u_k\rangle \langle u_k|, \quad (11.238)$$

where the set of eigenvectors  $\{u_k\}$  form an orthonormal basis set. Inserting Eq. 11.238 into Eq. 11.237 we obtain

$$C(t) = \sum_{k=1}^K d_k e^{-i\omega_k t}, \quad (11.239)$$

with

$$d_k \equiv |\langle u_k | \Phi_0 \rangle|^2, \quad (11.240)$$

which is identical with Eq. 11.236. In keeping with conventional quantum mechanics, we assume here that the Hamiltonian  $\hat{\Omega}$  is Hermitian, implying that both  $\omega_k$  and  $d_k$  are real with  $d_k > 0$ . In this special case the signal has time reversal symmetry:  $C(-t) = C^*(t)$ . Note though that in a more general formalism (see below) these assumptions are not necessary.

Equations 11.239–11.240 show the equivalence of the harmonic inversion problem to one of matrix diagonalization, reducing this centuries-old problem to a standard linear algebra calculation. For the case of a discrete time signal,  $C(t_n) = C(n\tau)$ , it is convenient to define the evolution operator for a single time step,  $\tau$ :

$$\hat{U} = e^{-i\tau\hat{\Omega}} = \sum_{k=1}^K e^{i\omega_k \tau} |u_k\rangle \langle u_k|. \quad (11.241)$$

Then  $e^{-it\hat{\Omega}} = \hat{U}^n$  and the discrete analog of Eq. 11.239 is

$$C(t_n) = C(n\tau) = \sum_{k=1}^K d_k e^{-i\omega_k n\tau}. \quad (11.242)$$

The remaining step is how to construct a two-dimensional array from the one-dimensional time signal  $c_n = C(n\tau)$ . Consider the Krylov-type basis

$$\Psi_j \equiv \Psi(z_j) = \sum_{n=0}^M \left( \hat{U}/z_j \right)^n \Phi_0, \quad (11.243)$$

for a set of complex values  $z_j \equiv e^{i\phi_j}$ ,  $j = 1, 2, \dots, N$  taken on the unit circle (real  $\phi_j$ ). The function  $\Psi(z_j)$  will be dominated by the eigenvectors  $|u_k\rangle$  whose eigenvalues  $u_k = e^{i\omega_k \tau}$  are close to  $z_j$ . This allows for control of the energy window of eigenvalues by the choice of  $\phi_j$ . The decomposition of the problem into separate energy bands by the choice of the  $\phi_j$  is known as filter diagonalization, which is an optional, but normally a desirable, component of the harmonic inversion scheme.

The matrix elements of the evolution operator in this Krylov-type basis take the form

$$U_{jj'} = \langle \Psi_j | \hat{U} | \Psi_{j'} \rangle. \quad (11.244)$$

Since the basis is not orthogonal we also need the overlap matrix

$$S_{jj'} = \langle \Psi_j | \Psi_{j'} \rangle. \quad (11.245)$$

Inserting Eq. 11.243 into Eqs. 11.244 and 11.245 we obtain

$$U_{jj'} = \sum_{n'=0}^M \sum_{n=0}^M c_{n-n'+1} z_j^{-n} z_{j'}^{n'} \quad (11.246)$$

$$S_{jj'} = \sum_{n'=0}^M \sum_{n=0}^M c_{n-n'} z_j^{-n} z_{j'}^{n'}. \quad (11.247)$$

The double sum in Eqs. 11.246–11.247 can be reduced to a single sum (see Eqs. 11.256–11.257 below for a similar but more general result). Although this simplifies the construction of the matrix  $U$ , it should not obscure the main point: Eq. 11.246 shows that the matrices  $U_{jj'}$  and  $S_{jj'}$  can be constructed from the one-dimensional sequence,  $c_n$ , allowing the use of matrix diagonalization techniques to solve the harmonic inversion problem.

Since the basis functions  $\{\Psi_j\}$  are generally not orthogonal, we must solve the generalized eigenvalue problem (see Exercises 8.79–8.80):

$$\mathbf{U} \mathbf{B}_k = u_k \mathbf{S} \mathbf{B}_k, \quad (11.248)$$

where the bold characters  $\mathbf{U}$  and  $\mathbf{S}$  define the corresponding matrices of size  $N \times N$ . The eigenvectors  $\mathbf{B}_k$  are then column vectors with elements  $B_{jk}$  satisfying

$$|u_k\rangle = \sum_{j=1}^K B_{jk} |\Psi_j\rangle. \quad (11.249)$$

Once we have the eigenvectors  $\mathbf{B}_k$  the amplitudes  $d_k$  can be obtained as

$$d_k \equiv |\langle u_k | \Phi_0 \rangle|^2 = \left| \sum_{j=1}^K B_{jk} \langle \Psi_j | \Phi_0 \rangle \right|^2. \quad (11.250)$$

To generalize the formalism to complex  $\{\omega_k\}$ , it is convenient to use a different convention for the inner product on the Hilbert space than we have used elsewhere in this book. Thus, instead of  $\langle u | \hat{A} | v \rangle \equiv \int_{-\infty}^{\infty} u^*(x) (\hat{A}v(x)) dx$  we use  $\langle u | \hat{A} | v \rangle \equiv \int_{-\infty}^{\infty} u(x) (\hat{A}v(x)) dx$ . Then

$$C(t) = \langle \Phi_0 | e^{-it\hat{\Omega}} | \Phi_0 \rangle \quad (11.251)$$

$$c_n = \langle \Phi_0 | \hat{U}^n | \Phi_0 \rangle = \langle \Phi_0 | e^{-int\hat{\Omega}} | \Phi_0 \rangle \quad (11.252)$$

$$\hat{U} = \sum_{k=1}^K u_k |u_k\rangle \langle u_k|. \quad (11.253)$$

Using the alternate inner product definition, the matrix elements of  $\hat{U}$  take the form

$$U_{jj'} = \sum_{n'=0}^M \sum_{n=0}^M c_{n+n'+1} z_j^{-n} z_{j'}^{-n'} = \sum_{n'=0}^M \sum_{n=0}^M (z_{j'}/z_j)^n c_{n+n'+1} z_{j'}^{-(n+n')} \quad (11.254)$$

and the overlap matrix has elements

$$S_{jj'} = \sum_{n'=0}^M \sum_{n=0}^M c_{n+n'} z_j^{-n} z_{j'}^{-n'} = \sum_{n'=0}^M \sum_{n=0}^M (z_{j'}/z_j)^n c_{n+n'} z_{j'}^{-(n+n')}. \quad (11.255)$$

Making the substitution  $l = n + n'$ , and summing over  $n$  one obtains

$$U_{jj'} = \frac{1}{z_j - z'_j} \left[ z_j \sum_{l=0}^M c_{l+p} z_{j'}^{-l} - z - j^{-M} \sum_{l=M+1}^{2M} c_{l+p} z_{j'}^{M-l+1} - z_{j'} \sum_{l=0}^M c_{l+p} z_j^{-l} + z_{j'}^{-M} \sum_{l=M+1}^{2M} c_{l+p} z_j^{M-l+1} \right] \quad (11.256)$$

$$U_{jj} = \sum_{l=0}^{2M} (M - |M - l| + 1) c_{l+p} z_j^{-l}, \quad (11.257)$$

with similar expressions for  $S_{jj'}$ .

To avoid spurious results, the time grid must be dense enough to adequately represent the maximum frequency contributing to the signal:

$$-\frac{\pi}{\tau} < \operatorname{Re} \omega_k < \frac{\pi}{\tau}, \quad (11.258)$$

Another condition, albeit not a very strict one, is on the imaginary part of  $\omega_k$ :

$$\operatorname{Im} \omega_k \leq O(N\tau). \quad (11.259)$$

This is also quite natural since it makes the signal  $C(t)$  bounded on the segment  $[0, N\tau]$ . We note, however, that in most physically interesting situations the dynamics are strictly dissipative, corresponding to all nonpositive  $\operatorname{Im} \omega_k$ . This is equivalent to having all the eigenvalues of  $\hat{U}$  inside the unit circle in the complex plane,  $|u_k| \leq 1$  (see Figure 11.10).

In a slightly different form, the harmonic inversion problem was already formulated two hundred years ago as a fit of a signal  $C(t)$  to the sum of purely exponentially decaying terms,

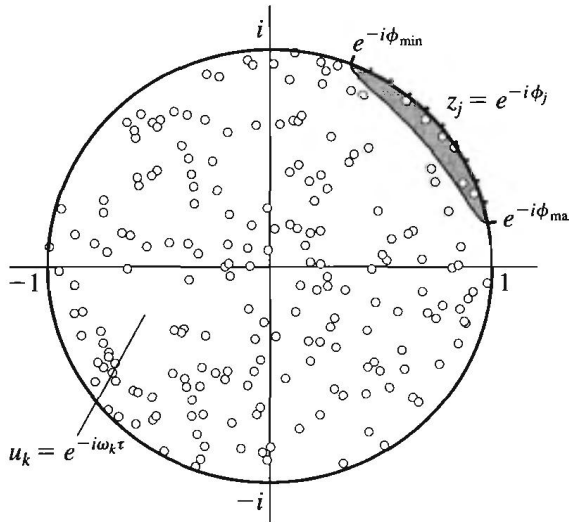


**Figure 11.10** A schematic plot of the eigenvalues of the operator  $\hat{U}$  for the case of strictly dissipative dynamics. Only a small portion (in the shadowed region) of the eigenvalues  $u_k$  are extracted by the filter-diagonalization procedure.

and an algorithm for its solution was discovered by Baron de Prony. There are several approaches related to the Prony method currently in use for extracting a high-resolution spectrum from short time signals, such as the modern versions of the Prony method, MUSIC, ESPRIT, and so forth. (see, e.g., Marple (1987); Roy (1991)). All these methods differ from the Fourier transform in that they are not based on a linear transformation of the signal and are in fact highly nonlinear by their nature. However, the common feature present in most versions of these methods is converting the nonlinear fitting problem to a linear algebra problem.

---

## Problems

► **Exercise 11.16** Show that the projection operator for the discrete  $k$ -basis can be written in the alternative, more symmetric forms:

$$P = P_{\Pi}(\hat{p})P_{\cup}(\hat{p})P_{\Pi}(\hat{p}) = P_{\cup}(\hat{p})P_{\Pi}(\hat{p})P_{\cup}(\hat{p}). \quad (11.260)$$

**Solution** These identities follow immediately from the fact that  $P_{\Pi}(\hat{p})$  and  $P_{\cup}(\hat{p})$  commute and the projection operator property  $P_{\Pi}(\hat{p})P_{\Pi}(\hat{p}) = P_{\Pi}(\hat{p})$  and  $P_{\cup}(\hat{p})P_{\cup}(\hat{p}) = P_{\cup}(\hat{p})$ .

► **Exercise 11.17** Use the Nyquist sampling theorem to show that

$$P_{\cup}(\hat{p})P_{\Pi}(\hat{x})P_{\cup}(\hat{p}) = P_{\cup}(\hat{p}) \quad P_{\cup}(\hat{x})P_{\Pi}(\hat{p})P_{\cup}(\hat{x}) = P_{\cup}(\hat{x}) \quad (11.261)$$

$$P_{\Pi}(\hat{p})P_{\cup}(\hat{x})P_{\Pi}(\hat{p}) = P_{\Pi}(\hat{p}) \quad P_{\Pi}(\hat{x})P_{\cup}(\hat{p})P_{\Pi}(\hat{x}) = P_{\Pi}(\hat{x}). \quad (11.262)$$

**Solution** The first identity follows by noting that  $P_{\cup}(\hat{p})$ , by sampling the wavefunction discretely in  $p$ -space, renders the function periodic in  $x$ -space. Making the function periodic in  $x$ , truncating it at the unit interval, and then making it again periodic in  $x$  is identical to making it periodic the first time around. The other identities can be arrived at by similar reasoning.

► **Exercise 11.18** Consider the operators  $P_{\Pi}(\hat{x})P_{\Pi}(\hat{p})$  and  $P_{\Pi}(\hat{x})P_{\cup}(\hat{p})$ . Do these operators satisfy the equation  $P^2 = P$ ? Are they Hermitian? Are they projection operators?

► **Exercise 11.19**

- a. Noting that the basis orthogonality relation, Eq. 11.155, can be rewritten as  $\Phi^\dagger \Phi = \mathbf{1}$ , find the corresponding grid orthogonality relation.
- b. Find the continuous analog of this discrete grid orthogonality relation.

**Solution**

- a. The grid orthogonality relation,  $\Phi \Phi^\dagger = \mathbf{1}$ , takes the form

$$\sum_{\kappa=-\frac{N}{2}+1}^{\frac{N}{2}} \Phi_\kappa(x_i) \Phi_\kappa^*(x_j) = \sum_{\kappa=-\frac{N}{2}+1}^{\frac{N}{2}} \frac{e^{\sqrt{-1}2\pi\kappa i/N}}{\sqrt{N}} \frac{e^{-\sqrt{-1}2\pi\kappa j/N}}{\sqrt{N}} = \delta_{ij}. \quad (11.263)$$

Equation 11.263 may be rewritten as

$$\sum_{\kappa=-\frac{N}{2}+1}^{\frac{N}{2}} \bar{\phi}_\kappa(x_i) \bar{\phi}_\kappa^*(x_j) \Delta k = \sum_{\kappa=-\frac{N}{2}+1}^{\frac{N}{2}} \frac{e^{\sqrt{-1}2\pi\kappa\Delta ki/2K}}{\sqrt{2K}} \frac{e^{-\sqrt{-1}2\pi\kappa\Delta kj/2K}}{\sqrt{2K}} \Delta k = \delta_{ij}. \quad (11.264)$$

where

$$\bar{\phi}_\kappa(x_j) = \frac{e^{-i2\pi\kappa\Delta kj/2K}}{\sqrt{2K}} \quad \text{and} \quad \Delta k = \frac{2K}{N}. \quad (11.265)$$

- b.** Equation 11.264 is the discrete version of the orthogonality relation

$$\int_{-K}^K \bar{\phi}_k(x_i) \bar{\phi}_k^*(x_j) dk = \int_{-K}^K \frac{e^{ik(x_i-x_j)}}{2K} dk = \delta_{ij}. \quad (11.266)$$

To see this, note that if  $i = j$  the integral gives 1. If  $i \neq j$  the integral gives

$$\int_{-K}^K \frac{e^{-ik(x_i-x_j)}}{2K} dk = \frac{e^{-ik(x_i-x_j)}}{-i(x_i - x_j)} \Big|_{-K}^K = \frac{e^{-i\pi(i-j)} - e^{i\pi(i-j)}}{-i(x_i - x_j)} = 0, \quad (11.267)$$

where we have used the relation  $K \Delta x = \pi$ . Equation 11.264 plays an important role in the Fourier Grid Hamiltonian method.

► **Exercise 11.20**

- a. Verify that Eq. 11.160 satisfies the basis orthogonality relation in Eq. 11.159.  
b. Find the corresponding grid orthogonality relation.

**Solution**

- a. Substitution of Eq. 11.160 into Eq. 11.159 yields

$$\sum_{j=-\infty}^{\infty} \frac{e^{i(k-k')x_j}}{2K} = \sum_{n=-\infty}^{\infty} \delta(k - k' - n2K) = \delta(k - k'), \quad (11.268)$$

where the first equality follows from Eq. 6.83 and the second equality follows from the restrictions  $-K \leq k, k' \leq K$ . Note that the pseudospectral “matrix,”  $\Phi_k(x_j)$ , has an infinite number of rows since the  $\{x_j\}$  are discrete but infinite, and an infinite number of columns since  $k$  is a continuous variable.

- b. To find the corresponding grid orthogonality relation we note that Eq. 11.159 can be written in matrix form as  $\Phi^\dagger \Phi = \mathbf{1}$ . The grid orthogonality relation,  $\Phi \Phi^\dagger = \mathbf{1}$ , takes the form

$$\int_{-K}^K \Phi_k(x_i) \Phi_k^*(x_j) dk = \int_{-K}^K \frac{e^{ik(x_i-x_j)}}{2K} dk = \delta_{ij}. \quad (11.269)$$

► **Exercise 11.21** Show that the complete set of sinc functions, Eq. 11.162, gives the same projector as that of Eq. 11.146.

**Solution** The sinc functions can be written in Dirac notation as

$$|\theta_j\rangle = P_{\sqcap}(\hat{p}) \frac{e^{-i\hat{p}x_j/\hbar}}{\sqrt{2K}} |0\rangle, \quad j = -\infty, \dots, \infty, \quad \Delta x = \frac{\pi}{K}, \quad (11.270)$$

where

$$P_{\sqcap}(p)\tilde{\Psi}(p) = \begin{cases} \tilde{\Psi}(p) & \text{if } p \in [-K, K] \\ 0 & \text{otherwise} \end{cases}$$

and

$$\langle x|0\rangle = \delta(0).$$

Forming the projection operator from Eq. 11.270 we obtain

$$P = \sum_{j=-\infty}^{\infty} |\theta_j\rangle\langle\theta_j| \quad (11.271)$$

$$= P_{\sqcap}(\hat{p}) \left( \sum_{j=-\infty}^{\infty} \frac{e^{-i\hat{p}x_j/\hbar}}{\sqrt{2K}} |0\rangle \left\langle 0 \middle| \frac{e^{i\hat{p}x_j/\hbar}}{\sqrt{2K}} \right. \right) P_{\sqcap}(\hat{p}) \quad (11.272)$$

$$= P_{\sqcap}(\hat{p}) \sum_{j=-\infty}^{\infty} |x_j\rangle\langle x_j| P_{\sqcap}(\hat{p}) \quad (11.273)$$

$$\equiv P_{\sqcap}(\hat{p}) P_{\sqcup}(\hat{x}) P_{\sqcap}(\hat{p}) \quad (11.274)$$

$$= P_{\sqcap}(\hat{p}), \quad (11.275)$$

where in the last line we have used Eq. 11.262.

► **Exercise 11.22** In the original formulation of filter diagonalization by Wall and Neuhauser, the basis functions are

$$\Psi_j = \int_{-\infty}^{\infty} e^{-iHt/\hbar} e^{i\omega_j t} e^{-\alpha t^2} \Phi_0 dt. \quad (11.276)$$

- a. Compare Eq. 11.276 with the spectral method for constructing eigenfunctions (Section 6.3). Discuss why  $\Psi_j$  will have significant components of only these eigenstates with energy in the range near  $\hbar\omega_j$ .
- b. Show that Eq. 11.243 is essentially the discrete counterpart of Eq. 11.276.
- c. Discuss why Eq. 11.243 represents a Krylov-type basis. In what way is it similar and in what way is it different from the standard Krylov basis discussed in Section 11.7.3?

---

## References

### General Numerical Methods, Gaussian Quadrature, Fast Fourier Transform

1. B. Carnahan, H. A. Luther and J. O. Wilkes, *Applied Numerical Methods* (Wiley, New York, 1969).
2. W. H. Press, B. P. Flannery, S. A. Teukolsky and W. T. Vetterling, *Numerical Recipes: The Art of Scientific Computing* (Cambridge University Press, 1986).
3. G. Strang, *Linear Algebra and Its Applications*, 3rd ed. (Harcourt Brace Jovanovich, San Diego, 1988).
4. E. Oran Brigham, *The Fast Fourier Transform* (Prentice Hall, Englewood Cliffs, NJ, 1974).
5. P. J. Davis and P. Rabinowitz, *Methods of Numerical Integration*, 2nd ed. (Academic Press, Orlando, 1984).
6. *Handbook of Mathematical Functions with Formulas, Graphs, and Mathematical Tables*, eds. M. Abramowitz and I. A. Stegun (National Bureau of Standards Applied Mathematics Series 55, 1964).

### Spectral and Pseudospectral Representation

7. D. Gottlieb and S. A. Orszag, *Numerical Analysis of Spectral Methods: Theory and Application* (SIAM, Philadelphia, 1977).

### Gaussian Quadrature via Matrix Diagonalization

8. D. O. Harris, G. G. Engerholm and W. D. Gwinn, Calculation of matrix elements for one-dimensional quantum-mechanical problems and the application to anharmonic oscillators, *J. Chem. Phys.* 43, 151 (1965).
9. A. S. Dickinson and P. R. Certain, Calculation of matrix elements for one-dimensional quantum-mechanical problems, *J. Chem. Phys.* 49, 4209 (1968).
10. G. H. Golub and J. H. Welsch, Calculation of Gauss quadrature rules, *Math. Comp.* 23, 221 (1969).
11. I. Degani, J. Schiff and D. J. Tannor, Commuting extensions and cubature formulae, *Numerische Mathematik* (2005).

### Discrete Variable Representation

12. J. C. Light, I. P. Hamilton and J. V. Lill, Generalized discrete variable approximation in quantum mechanics, *J. Chem. Phys.* 82, 1400 (1985).
13. J. C. Light, Discrete variable representations in quantum dynamics, in *Time Dependent Quantum Molecular Dynamics*, eds. J. Broeckhove and L. Lathouwers (Plenum, New York, 1992), p. 185.
14. R. G. Littlejohn, M. Cargo, T. Carrington, Jr., K. A. Mitchell and B. Poirier, A general framework for discrete variable representation basis sets, *J. Chem. Phys.* 116, 8691 (2002).
15. J. C. Light and T. Carrington, Jr., Discrete variable representations and their utilization, *Adv. Chem. Phys.* 114, 263 (2000).
16. R. Dawes and T. Carrington, Jr., A multidimensional discrete variable representation basis obtained by simultaneous diagonalization, *J. Chem. Phys.* 121, 726 (2004).

## Phase Space Representation

17. M. J. Davis and E. J. Heller, Semiclassical Gaussian basis set method for molecular vibrational wave functions, *J. Chem. Phys.* 71, 3383 (1979).
18. R. Kosloff, Time-dependent quantum-mechanical methods for molecular dynamics, *J. Phys. Chem.* 92, 2087 (1988).
19. E. Fattal, R. Baer and R. Kosloff, Phase space approach for optimizing grid representations: The mapped Fourier method, *Phys. Rev. E* 53, 1217 (1996).
20. B. Poirier, Algebraically self-consistent quasiclassical approximation on phase space, *Found. Phys.* 30, 1191 (2000); B. Poirier and J. C. Light, Phase space optimization of quantum representations: Direct product basis sets, *J. Chem. Phys.* 111, 4869 (1999); B. Poirier and J. C. Light, Phase space optimization of quantum representations: Three-body systems and the bound states of HCO, *J. Chem. Phys.* 113, 211 (2000).

## Fourier Method

21. D. Kosloff and R. Kosloff, A Fourier method solution for the time dependent Schrödinger equation as a tool in molecular dynamics, *J. Comput. Phys.* 52, 35 (1983); R. Kosloff and D. Kosloff, A Fourier method solution for the time dependent Schrödinger equation: A study of the reaction  $\text{H}^+ + \text{H}_2$ ,  $\text{D}^+ + \text{HD}$ , and  $\text{D}^+ + \text{H}_2$ , *J. Chem. Phys.* 79, 1823 (1983).
22. M. D. Feit, J. A. Fleck, Jr. and A. Steiger, Solution of the Schrödinger equation by a spectral method, *J. Comput. Phys.* 47, 412 (1982); M. D. Feit and J.A. Fleck, Jr., Solution of the Schrödinger equation by a spectral method II: Vibrational energy levels of triatomic molecules, *J. Chem. Phys.* 78, 301 (1983); M. D. Feit and J. A. Fleck, Jr., Wavepacket dynamics and chaos in the Hénon-Heiles system, *J. Chem. Phys.* 80, 2578 (1984).
23. R. Kosloff, Time dependent methods in molecular dynamics, *J. Phys. Chem.* 92, 2087 (1988).
24. R. Kosloff, The Fourier method, in *Numerical Grid Methods and Their Application to Schrödinger's Equation*, ed. C. Cerjan (Kluwer, Boston, 1993).
25. C. C. Marston and G. G. Balint-Kurti, The Fourier grid Hamiltonian method for bound state eigenvalues and eigenfunctions, *J. Chem. Phys.* 91, 3571 (1989).
26. D. T. Colbert and W. H. Miller, A novel discrete variable representation for quantum mechanical reactive scattering via the *S*-matrix Kohn method, *J. Chem. Phys.* 96, 1982 (1992).

## Mapped Fourier Method

27. F. Gygi, Adaptive Riemannian metric for plane-wave electronic-structure calculations, *Europhys. Lett.* 19, 617 (1992).
28. E. Fattal, R. Baer and R. Kosloff, Phase space approach for optimizing grid representations: The mapped Fourier method, *Phys. Rev. E* 53, 1217 (1996).
29. V. Kokououline, O. Dulieu, R. Kosloff and F. Masnou-Seeuws, Mapped Fourier methods for long-range molecules: Application to perturbations in the  $\text{Rb}_2$  ( $\text{O}_u^+$ ) photoassociation spectrum, *J. Chem. Phys.* 110, 9865 (1999).
30. Y. Goldfarb and D. J. Tannor, in preparation.
31. K. Willner, O. Dulieu and F. Masnou-Seeuws, Mapped grid methods for long-range molecules and cold collisions, *J. Chem. Phys.* 120, 548 (2004).

## Time Propagation

32. *Time Dependent Methods for Quantum Dynamics*, ed. K. C. Kulander, *Comput. Phys. Commun.* 63 (1991).
33. *Time Dependent Quantum Molecular Dynamics*, eds. J. Broeckhove and L. Lathouwers (Plenum, New York, 1992).

34. E. A. McCullough, Jr. and R. E. Wyatt, Dynamics of the collinear H + H<sub>2</sub> reaction. I. Probability density and flux, *J. Chem. Phys.* 54, 3578 (1971).
35. A. Askar and A. S. Cakmak, Explicit integration method for the time-dependent Schrödinger equation for collision problems, *J. Chem. Phys.* 68, 2794 (1978).
36. M. D. Feit, J. A. Fleck, Jr. and A. Steiger, Solution of the Schrödinger equation by a spectral method, *J. Comput. Phys.* 47, 412 (1982).
37. H. Tal-Ezer and R. Kosloff, An accurate and efficient scheme for propagating the time dependent Schrödinger equation, *J. Chem. Phys.* 81, 3967 (1984).
38. T. J. Park and J. C. Light, Unitary quantum time evolution by iterative Lanczos reduction, *J. Chem. Phys.* 85, 5870 (1986).
39. C. Leforestier et al., A comparison of different propagation schemes for the time dependent Schrödinger equation, *J. Comput. Phys.* 94, 59 (1991).
40. P. Schwendner, F. Seyl and R. Schinke, Photodissociation of Ar<sub>2</sub><sup>+</sup> in strong laser fields, *Chem. Phys.* 217, 233 (1997).
41. R. Kosloff, Propagation methods for quantum molecular dynamics, *Ann. Rev. Phys. Chem.* 45, 145 (1994).
42. S. K. Gray and D. E. Manolopoulos, Symplectic integrators tailored to the time-dependent Schrödinger equation, *J. Chem. Phys.* 104, 7099 (1996).

### Spectral Analysis of Time Signals

43. S. Marple, Jr., *Digital Spectral Analysis with Applications*, Prentice Hall, Englewood Cliffs, NJ, 1987.
44. R. Roy, B. G. Sumpter, G. A. Pfeffer, S. K. Gray and D. W. Noid, Novel methods for spectral analysis, *Comput. Phys. Rep.* 205, 109 (1991).
45. M. R. Wall and D. Neuhauser, Extraction, through filter diagonalization, of general quantum eigenvalues or classical normal mode frequencies from a small number of residues or a short-time segment of a signal. I. Theory and application to a quantum-dynamics model, *J. Chem. Phys.* 102, 8011 (1995).
46. D. Neuhauser, Bound state eigenfunctions from wavepackets: Time → energy resolution, *J. Chem. Phys.* 93, 2611 (1990).
47. V. A. Mandelshtam and H. S. Taylor, A low-storage filter diagonalization method for quantum eigenenergy calculation or for spectral analysis of time signals, *J. Chem. Phys.* 106, 5085 (1997).
48. V. A. Mandelshtam and H. S. Taylor, Spectral analysis of time correlation function for a dissipative dynamical system using filter diagonalization: Application to calculation of unimolecular decay rates, *Phys. Rev. Lett.* 78, 3274 (1997).